

Reduced basis approximation of parametric eigenvalue problems in presence of clusters and intersections

Daniele Boffi^{K,P}, Abdul Halim^{K,H}, and Gopal Priyadarshi^{K,PP}

^KKing Abdullah University of Science and Technology, Saudi Arabia

^PDipartimento di Matematica “F. Casorati”, University of Pavia, Italy

^HDepartment of Mathematics, Hari Singh College, Munger University, India

^{PP}Department of Mathematics, S.M.D. College, Patliputra University, India

February 3, 2023

Abstract

In this paper we discuss reduced order models for the approximation of parametric eigenvalue problems. In particular, we are interested in the presence of intersections or clusters of eigenvalues. The singularities originating by these phenomena make it hard a straightforward generalization of well known strategies normally used for standard PDEs. We investigate how the known results extend (or not) to higher order frequencies.

1 Introduction

Reduced order methods are nowadays a classical tool for the efficient and effective approximation of partial differential equations. The interested reader is referred, for instance, to the monographs [17, 8] and to the references therein.

We aim to investigate the use of reduced order models for the approximation of parametric eigenvalue problems. In the pioneer works [11, 10] and [15, 16] the approximation of the first fundamental mode was explored. Investigations for higher (isolated) modes started in [13, 12, 14]. In [3] we exploited an idea originating from [4, 7] of adding a fictitious time variable for the solution of a non parametric eigenvalue problem.

The state of the art of the theory concerning reduced basis approximation of parametric eigenvalue problems stems from the results of [5] and [9]. In particular, [5] deals with the first isolated eigenvalue, while [9] approximates at once a fixed number of eigenmodes, with eigenvalues separated from the rest of the spectrum, starting from the first one. From those papers it is clear that trouble can come from the intersection of eigenvalues or when eigenvalues are not well separated from each other. Some preliminary discussion about these issues and about the tracking of different modes is contained in [1, 2] and an example of application to the Maxwell eigenvalue problem has been investigated in [6].

In this paper we are highlighting problematic situations, with the hope that these investigations can open the way towards robust solutions to the presented issues. For this reason, we will discuss rather simple examples where the parametric space is one or two dimensional.

After examining examples where the results of [5] and [9] are confirmed, we investigate the situation when higher frequencies are looked for. For instance, a naive generalization of [5] would deal with an isolated eigenvalue which is not the first fundamental one. Analogously, a direct generalization of [9] involves a cluster of eigenvalues well separated from the rest of the

spectrum which does not contain the first fundamental mode. At a first glance we were surprised by the obtained results, even if there are clear explanations for the fact that the conclusions of [5] and [9] do not extend trivially to higher modes. As a side note, we also try to suggest cheaper solutions for the simultaneous approximation of the first eigenmodes presented in [9]. We also show how the obtained solutions can be sensitive to the dimension of the POD reduced basis.

We are confident that the presented results will be useful for future investigations with the aim of optimizing the strategy for the approximation of parametric eigenvalue problems.

In Section 2 we present the general setting of our elliptic parametric eigenvalue problem, together with its finite element discretization and the standard approach for the construction of a reduced order model based on POD and reduced basis. In Section 4 we describe the main outcomes of our investigations, which are reported in Section 5 and 6 for the one and two dimensional cases, respectively.

2 Problem setting

2.1 Parametric elliptic eigenvalue problem

Let $\Omega \subset \mathbb{R}^2$ be a bounded and polygonal domain and $\mu \in \mathcal{M} \subset \mathbb{R}^P$, where \mathcal{M} is the parameter space. Our goal is to find $(\lambda(\mu), u(\mu))$ such that

$$\begin{cases} -\operatorname{div}(A(\mu)\nabla u(\mu)) = \lambda(\mu)u(\mu) & \text{in } \Omega \\ u(\mu) = 0 & \text{on } \partial\Omega, \end{cases} \quad (2.1)$$

where the diffusion matrix $A(\mu) \in \mathbb{R}^{2 \times 2}$ is symmetric and positive definite for all values of the parameter μ .

It is well known from the theory of compact elliptic eigenvalue problems that the above problem is well-posed and all the eigenvalues are strictly positive.

It is also well known that the regularity of the eigenmodes in terms of the parameter μ play a crucial role for the study of the solution. In particular, in this paper we are interested in those parametric eigenvalue problems where intersecting eigenvalue phenomena occur. We have initiated some discussion about this issue in [1] and we go deeper into it in this work.

2.2 Finite element approximation

The finite element approximation of (2.1) is based on the following variational formulation. Let V be the Sobolev space $H_0^1(\Omega)$ and $a, m : V \times V \times \mathcal{M} \rightarrow \mathbb{R}$ be the parameter dependent bilinear forms defined by

$$\begin{aligned} a(u, v; \mu) &= \int_{\Omega} (A(\mu)\nabla u(\mu)) \cdot \nabla v \, dx \\ m(u, v; \mu) &= \int_{\Omega} u(\mu)v \, dx. \end{aligned} \quad (2.2)$$

The weak formulation of (2.1) is defined as: given $\mu \in \mathcal{M}$, find $(\lambda(\mu), u(\mu)) \in \mathbb{R}_+ \times V \setminus \{0\}$ such that

$$a(u, v; \mu) = \lambda(\mu)m(u, v; \mu) \quad \forall v \in V. \quad (2.3)$$

We note that $a(\bullet, \bullet; \mu)$ is symmetric and coercive, with coercivity constant depending on the Poincaré constant and on μ , and that $m(\bullet, \bullet; \mu)$ coincides with the $L^2(\Omega)$ -inner product for all μ . Actually, our setting would allow for a varying bilinear form on the right hand side of (2.3) even if in our examples we take it constant.

Let us consider the finite element subspace $V_h \subset V$ of dimension N_h

$$V_h = \{v_h \in C^0(\bar{\Omega}) : v_h|_K \in \mathbb{P}_1(K) \ \forall K \in \mathcal{T}_h \ v_h|_{\partial\Omega} = 0\},$$

where \mathcal{T}_h is a conforming triangulation of Ω with N_h internal vertices and $\mathbb{P}_1(K)$ is the set of polynomials with degree less than or equal to one on $K \in \mathcal{T}_h$. The finite element or *high fidelity* problem is defined as: given $\mu \in \mathcal{M}$, find $(\lambda_h(\mu), u_h(\mu)) \in \mathbb{R}_+ \times V_h \setminus \{0\}$ such that

$$a(u_h, v_h; \mu) = \lambda_h(\mu)m(u_h, v_h; \mu) \quad \forall v_h \in V_h. \quad (2.4)$$

Let $\{\phi_i\}_{i=1}^{N_h}$ be a basis of V_h , then the finite element solution $u_h(\mu)$ can be expressed as

$$u_h(\mu) = \sum_{i=1}^{N_h} u_h^i(\mu) \phi_i$$

where $\{u_h^i(\mu)\}_{i=1}^{N_h}$ are the finite element coefficients. Substituting the expression of $u_h(\mu)$ in (2.4), we obtain the following linear algebraic equation

$$A_h(\mu)U_h(\mu) = \lambda_h(\mu)M_h(\mu)U_h(\mu)$$

where the stiffness matrix A_h and mass matrix M_h are given by

$$(A_h(\mu))_{i,j} = a(\phi_j, \phi_i; \mu)$$

$$(M_h(\mu))_{i,j} = m(\phi_j, \phi_i; \mu)$$

with $i, j = 1, 2, \dots, N_h$ and where $U_h(\mu)$ is the column vector formed by the finite element coefficients.

3 Reduced basis approach

In the last few years, reduced basis method has emerged as a very powerful method to solve parameterized PDEs. In this method, the original PDE is projected onto a reduced subspace whose basis is obtained from the high fidelity solution evaluated at few suitable sample points.

We start with a set of finite element solutions for various values of the parameter μ , the so called snapshots, and generate a set of N basis functions, the so called reduced basis, $\{\zeta_1, \zeta_2, \dots, \zeta_N\}$. We define the N -dimensional reduced basis space as follows

$$V_N = \text{span}\{\zeta_i : i = 1, 2, \dots, N\}.$$

There are mainly two approaches based on which reduced basis can be constructed. The first one is the so called greedy approach in which snapshot vectors are chosen based on a posteriori error estimator, whereas the other approach is the proper orthogonal decomposition (POD) in which the reduced basis is chosen based on a singular value decomposition of the snapshot matrix. In our discussion we are going to follow the latter approach.

The reduced basis eigenvalue problem is given by: for $\mu \in \mathcal{M}$, find $(\lambda_N(\mu), u_N(\mu)) \in \mathbb{R}_+ \times V_N \setminus \{0\}$, such that

$$a(u_N, v_N; \mu) = \lambda_N(\mu)m(u_N, v_N; \mu) \quad \forall v_N \in V_N. \quad (3.1)$$

Since $\{\zeta_i\}_{i=1}^N$ form a basis for the reduced space V_N , any $u_N \in V_N$ can be expressed as

$$u_N(\mu) = \sum_{i=1}^N u_N^i(\mu) \zeta_i,$$

where $\{u_N^i(\mu)\}_{i=1}^N$ are the reduced basis coefficients. Substituting the expression of $u_N(\mu)$ in (3.1), we obtain the following linear algebraic equation

$$A_N(\mu)U_N(\mu) = \lambda_N(\mu)M_N(\mu)U_N(\mu),$$

where

$$(A_N(\mu))_{i,j} = a(\zeta_j, \zeta_i; \mu) \text{ and } (M_N(\mu))_{i,j} = m(\zeta_j, \zeta_i; \mu) \quad (i, j = 1, 2, \dots, N) \quad (3.2)$$

and where $U_N(\mu)$ is the column vector of the reduced basis coefficients.

Remark 3.1. In the above discussion it is hidden a crucial difference between the analysis of eigenvalue problems and source problems. Namely, in a typical source problem there is only one high fidelity solution associated with the source term and any reduced order model is trying to approximate that unique solution. However, an eigenvalue problem has typically infinitely many solutions: in our case, a sequence of increasing eigenvalues which correspond to (finite dimensional) eigenspaces. The high fidelity problem (2.4) has N_h solutions (counted with their multiplicities) and the classical theory guarantees that, for h small enough, the k -th discrete eigenvalue $\lambda_{h,k}(\mu)$ converges to the corresponding continuous one $\lambda_k(\mu)$. Analogously, the discrete eigenfunctions converge to the continuous ones, according to a definition that should take into account the multiplicity of the eigenspaces and the fact that convergence involves the entire eigenspace and not just a basis of it (typically the definition of convergence is stated in terms of the gap between subspaces of a Hilbert space).

It turns out, first of all, that the choice of snapshots should take into account which eigenmode(s) we want to approximate. After the choice of the reduced basis, the reduced problem (3.1) has N solutions (counted with their multiplicities) and the main question is whether the k -th eigenmode of (3.1) has some similarity with the ℓ -th eigenmode of (2.4) and, if so, for what values of k and ℓ .

3.1 Relation between the reduced and the high fidelity systems

Since $V_N \subset V_h$, the reduced basis ζ_i can be written in terms of the finite element basis as

$$\zeta_i = \sum_{j=1}^{N_h} \zeta_i^j \phi_j, \quad i = 1, \dots, N. \quad (3.3)$$

Let us denote by $\boldsymbol{\zeta}_i = (\zeta_i^1, \dots, \zeta_i^{N_h})^\top \in \mathbb{R}^{N_h}$ the nodal vectors corresponding to the basis ζ_i and let us consider the matrix

$$\mathbb{V} = [\boldsymbol{\zeta}_1 | \dots | \boldsymbol{\zeta}_N] \in \mathbb{R}^{N_h \times N}.$$

Using the expression (3.3) we have

$$a(\zeta_p, \zeta_q; \mu) = \sum_{i=1}^{N_h} \sum_{j=1}^{N_h} \zeta_p^j a(\phi_j, \phi_i; \mu) \zeta_q^i, \quad m(\zeta_p, \zeta_q; \mu) = \sum_{i=1}^{N_h} \sum_{j=1}^{N_h} \zeta_p^j m(\phi_j, \phi_i; \mu) \zeta_q^i,$$

for any $1 \leq p, q \leq N$.

Thus, we have the following relation between the matrices of the high fidelity and of the reduced systems

$$A_N(\mu) = \mathbb{V}^\top A_h(\mu) \mathbb{V}, \quad M_N(\mu) = \mathbb{V}^\top M_h(\mu) \mathbb{V}.$$

3.2 Online/offline paradigm

In order to develop computationally efficient reduced order models, we need some further assumptions on our parametric bilinear forms. We assume as usual that the bilinear forms $a(\bullet, \bullet; \mu)$ and $m(\bullet, \bullet; \mu)$ are affine dependent from the parameter, i.e.

$$a(\bullet, \bullet; \mu) = \sum_{k=1}^S \theta_k(\mu) a_k(\bullet, \bullet)$$

and

$$m(\bullet, \bullet; \mu) = \sum_{k=1}^Q \Theta_k(\mu) m_k(\bullet, \bullet),$$

where the bilinear forms $a_k(\bullet, \bullet)$ and $m_k(\bullet, \bullet)$ are parameter independent. Hence, these bilinear forms can be assembled only once for all the computations, which leads to a huge computational reduction in the reduced order method.

Let A_h^k and M_h^k be the matrices corresponding to the bilinear forms $a_k(\bullet, \bullet)$ and $m_k(\bullet, \bullet)$, respectively, then the matrix form for the high fidelity problem will be

$$A_h(\mu) = \sum_{k=1}^S \theta_k(\mu) A_h^k, \quad M_h(\mu) = \sum_{k=1}^Q \Theta_k(\mu) M_h^k$$

and the matrices corresponding to the reduced system will be

$$A_N(\mu) = \sum_{k=1}^S \theta_k(\mu) A_N^k = \sum_{k=1}^S \theta_k(\mu) \mathbb{V}^\top A_h^k \mathbb{V}, \quad M_N(\mu) = \sum_{k=1}^Q \Theta_k(\mu) M_N^k = \sum_{k=1}^Q \Theta_k(\mu) \mathbb{V}^\top M_h^k \mathbb{V}.$$

Since the matrices $\mathbb{V}^\top A_h^k \mathbb{V}$ and $\mathbb{V}^\top M_h^k \mathbb{V}$ are parameter independent, these are calculated in the offline stage and in the online stage the reduced matrices are formed by just evaluating the parameter dependent function θ_k ($k = 1, \dots, S$) and Θ_k ($k = 1, \dots, Q$) at the given parameter μ . Hence, in the online stage we only have to solve the reduced system.

3.3 Construction of the POD basis functions

In this subsection we recall the standard technique for the construction of the reduced basis using POD.

Given a snapshot matrix $S = [\mathbf{s}_1 | \dots | \mathbf{s}_{N_s}]$ of N_s snapshots, we want to find a reduced basis ζ_1, \dots, ζ_N ($N \ll N_h$) that spans the reduced space V_N . The reduced basis can be obtained using the SVD of the snapshot matrix. Applying the SVD to the snapshot matrix S , we get

$$S = W \Sigma Z^\top \tag{3.4}$$

where

$$W = [\zeta_1, \dots, \zeta_{N_h}] \in \mathbb{R}^{N_h \times N_h} \quad \text{and} \quad Z = [\psi_1, \dots, \psi_{N_s}] \in \mathbb{R}^{N_s \times N_s}$$

are orthogonal matrices and $\Sigma = \text{diag}(\sigma_1, \dots, \sigma_r, 0, \dots, 0) \in \mathbb{R}^{N_h \times N_s}$ contains the singular values of S with $\sigma_1 \geq \sigma_2 \geq \dots \geq \sigma_r > 0$, where r is the rank of the matrix S . The columns of W are the left singular vectors of S , the columns of the matrix Z are the right singular vectors of S , and $\sigma_1, \dots, \sigma_r$ are the singular values of S . The first N columns of W are the best choice for the N dimensional basis. The meaning of this claim is that this choice minimizes the sum of squares of the errors between each snapshot vector \mathbf{s}_i and its projection onto any N -dimensional subspace; this is a consequence of the Schmidt–Eckart–Young theorem which we recall for the readers convenience.

Theorem 3.2 (Schmidt–Eckart–Young. See [17]). *Given a matrix $S \in \mathbb{R}^{N_h \times N_s}$ of rank r , the matrix*

$$S_k = \sum_{i=1}^k \sigma_i \boldsymbol{\zeta}_i \boldsymbol{\psi}_i^\top \quad (1 \leq k \leq r)$$

satisfies the optimality property

$$\|S - S_k\|_F = \min_{\substack{B \in \mathbb{R}^{N_h \times N_s} \\ \text{rank}(B) \leq k}} \|S - B\|_F = \sqrt{\sum_{i=k+1}^r \sigma_i^2}, \quad (3.5)$$

where $\|\cdot\|_F$ is the Frobenius matrix norm.

In general, $N_h \gg N_s$ and the following procedure can be adopted in order to compute the reduced basis, that is the first N left singular vectors. From (3.4) we deduce

$$SZ = W\Sigma \quad \text{and} \quad S^\top W = Z\Sigma^\top \quad (3.6)$$

and we can write

$$S\boldsymbol{\psi}_i = \sigma_i \boldsymbol{\zeta}_i \quad \text{and} \quad S^\top \boldsymbol{\zeta}_i = \sigma_i \boldsymbol{\psi}_i \quad i = 1, \dots, r. \quad (3.7)$$

The first relation of (3.7) gives

$$\boldsymbol{\zeta}_i = \frac{1}{\sigma_i} S\boldsymbol{\psi}_i \quad i = 1, \dots, r. \quad (3.8)$$

Using (3.8) in the second relation of (3.7) we get

$$S^\top S\boldsymbol{\psi}_i = \sigma_i^2 \boldsymbol{\psi}_i \quad i = 1, \dots, r. \quad (3.9)$$

Thus we need to find the first N eigenvectors corresponding to the largest eigenvalues of the symmetric matrix $S^\top S \in \mathbb{R}^{N_s \times N_s}$. Once we find the right eigenvectors $\boldsymbol{\psi}_i$ ($i = 1, \dots, N$) we get the first N left eigenvectors using (3.8). The advantage of this procedure is that we need to find eigenvalues of a matrix whose size is $N_s \ll N_h$. The matrix $S^\top S$ is called correlation or Gram matrix.

Remark 3.3. In this paper, we consider snapshot matrices using different eigenvectors and their combinations at the sample parameters (see also Remark 3.1). For example, we consider a snapshot matrix S using the first three eigenvectors at the sample points $\mu_1, \mu_2, \dots, \mu_{n_s}$, that is

$$S = [u_{1,h}(\mu_1)|u_{2,h}(\mu_1)|u_{3,h}(\mu_1)|u_{1,h}(\mu_2)|\dots|u_{3,h}(\mu_{n_s})].$$

In this case $N_s = 3n_s$, and the columns are renamed as \boldsymbol{s}_i , $i = 1, 2, \dots, N_s$.

From the above discussion it is clear that a crucial aspect will be the selection of the reduced basis dimension N . A viable strategy consists in selecting a tolerance ϵ_{tol} and in using the following formula.

Choose N as the smallest integer such that

$$\frac{\sum_{i=1}^N \sigma_i^2}{\sum_{i=1}^r \sigma_i^2} \geq 1 - \epsilon_{tol} \quad (3.10)$$

where r is the rank of the snapshot matrix.

A reasonable choice for our computations seems to be $\epsilon_{tol} = 10^{-8}$. However, within the same example, we might vary N in order to see how the results are sensitive to this choice.

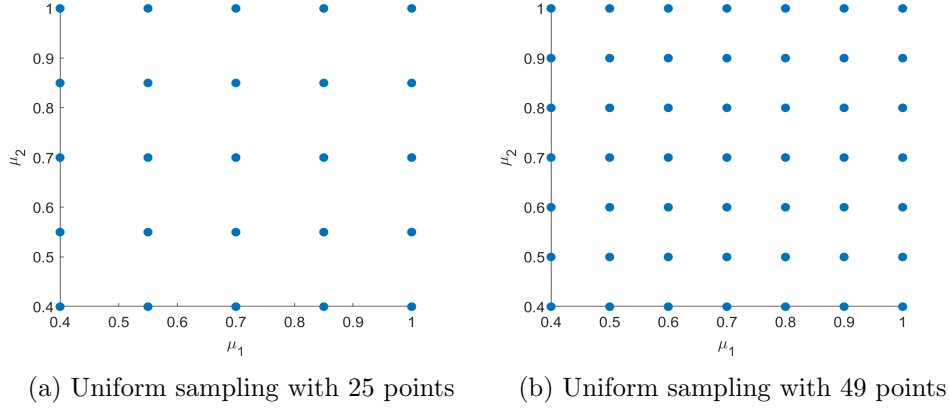


Figure 1: Uniform sampling of the parameter domain $[0.4, 1]^2$ with 25 and 49 points.

3.4 Parameter sampling technique

The sampling of the parametric space is very important for the success of reduced order modeling, especially when the dimension of the parameter domain is high and where curse of dimensionality should be tackled. There are several techniques for sampling the parameters such as uniform tensorial grid, Latin hypercube sampling, random sampling, sparse Smolyak sampling with Clenshaw-Curtis points, Monte-Carlo sampling, etc. LHS sampling is a special type of random sampling. In this paper we used uniform sampling as the focus of the paper is to investigate the behavior of reduced order model in relation to the choice of eigenfunctions for the construction of the snapshot matrix.

In Figure 1 we have displayed the sample points with blue dots using a uniform sampling technique for the parameter domain $\mathcal{M} = [0.4, 1]^2$. Four test points are used for testing the results of our reduced order model (ROM) in Subsection 6.

4 Overview of the numerical investigations

We want to investigate numerically the behavior of POD based ROM methods for the approximation of parametric eigenvalue problems in which intersecting eigenvalue phenomena occur. Our main questions are the following ones:

1. How to form the snapshot matrix? Which eigenfunctions should be included in presence of crossings?
2. How to choose the dimension N of the reduced basis?
3. Is it always the case that if N is large (eventually up to the size of the snapshot matrix) then the solutions of the reduced model converge towards the high fidelity solutions?

From the analysis of the existing literature and from our intuition we were expecting the following behavior related to question number 1.

- a) If we want to approximate an eigenmode with an eigenvalue $\lambda(\mu)$ which has no intersections with other modes in the range of the parameter $\mu \in \mathcal{M}$, then the snapshot matrix could be computed by using only high fidelity eigenfunctions associated with $\lambda(\mu)$.

- b) If we want to approximate an eigenmode with an eigenvalue that has intersections with other eigenvalues and if all these eigenvalues are well separated from the rest of the spectrum in the range of the parameter $\mu \in \mathcal{M}$, then the snapshot matrix should be computed by considering high fidelity eigenfunctions associated with all the modes that cross each other.

Concerning question number 2 we thought that the heuristic strategy described with formula (3.10) could be a good starting point for our numerical tests. Consequently, we were expecting the following behavior in connection with question number 3 depending on whether we are in presence of cases a) or b) above.

- a) The first eigenvalue of the reduced system converges toward the isolated high fidelity eigenvalue $\lambda(\mu)$ as N increases. The same applies to the corresponding eigenspace.
- b) If there are k eigenmodes belonging to the cluster that we are considering, then the first k eigenvalues of the reduced system converge towards the eigenvalues of interest of the high fidelity problem. The same applies to the corresponding eigenspaces.

The results of our computation are in agreement with our expectations *provided we are dealing with the first eigenvalues in the spectrum*. This means that things work well in case a) if $\lambda(\mu)$ is the first fundamental mode for all values of $\mu \in \mathcal{M}$. We will see that things may go wrong if we form the snapshot matrix of an isolated eigenmode which is not the first one. Analogously, in presence of clusters of k eigenvalues, it is in general a good strategy to form the snapshot matrix by considering all the corresponding eigenfunctions if we are dealing with the first k eigenmodes (with possible crossings). On the other hand, things may go wrong if we perform the same strategy with clusters in the higher part of the spectrum.

We point out that this behavior is in perfect agreement with the theoretical results of [5] (first isolated eigenvalue) and [9] (first k eigenvalues isolated from the next ones). However, our computations show that these results cannot be generalized to higher order modes.

To deal with these problems, we consider all n eigenfunctions (corresponding to the first smallest n eigenvalues) simultaneously in the snapshot matrix in order to obtain the first smallest n eigenvalues. It is shown through various examples that using this strategy the reduced order method provides all n eigenvalues (whether intersecting or non-intersecting) and the corresponding eigenfunctions correctly. It is also shown that as we increase the ROM dimension, eigenvalue based on ROM converge to the eigenvalue obtained through finite element approximation.

If we are interested in finding the first n eigenvalues, then putting all the n eigenvectors in the snapshot matrix at the sample points, we get good results which also maintain the order of the eigenvalues but the number of snapshots increased by multiple of n . In order to reduce the size of the snapshot matrix, we consider the following **alternate** strategy for getting the first n eigenvalues simultaneously. Instead of taking all the n eigenvectors, we choose some linear combination

$$\tilde{u}(\mu) = c_1 u_1(\mu) + \cdots + c_n u_n(\mu) \quad (c_j \neq 0 \forall j)$$

of them in the snapshot matrix. Our tests show that this can be a cheaper alternative in order to compute n simultaneous approximations of the eigenvalues and of the corresponding eigenfunctions in the correct order. In our numerical tests we use the sum of the first n eigenfunctions in the snapshot matrix.

We present two sets of numerical examples: the first one is for a one dimensional parameter space and the second one is for a two dimensional parameter space.

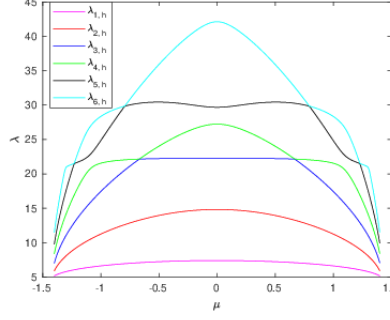


Figure 3: First six sorted eigenvalues when $h = 0.05$ and $\mu = -1.4 : 0.01 : 1.4$.

5 Numerical results for eigenvalue problems depending on one parameter

We consider the following eigenvalue problem: for $\mu \in (-\sqrt{2}, \sqrt{2})$, find $(\lambda(\mu), u(\mu)) \in \mathbb{R}^+ \times V \setminus \{0\}$ such that

$$\begin{cases} -\operatorname{div}(A(\mu)\nabla u(\mu)) = \lambda(\mu)u(\mu) & \text{in } \Omega = (-1, 1)^2 \\ u(\mu) = 0 & \text{on } \partial\Omega, \end{cases} \quad (5.1)$$

where the diffusion matrix $A(\mu) \in \mathbb{R}^{2 \times 2}$ is given by

$$A(\mu) = \begin{bmatrix} 1 & \mu \\ \mu & 2 \end{bmatrix}.$$

It is easy to check that A is symmetric and its eigenvalues are strictly greater than zero when $-\sqrt{2} < \mu < \sqrt{2}$.

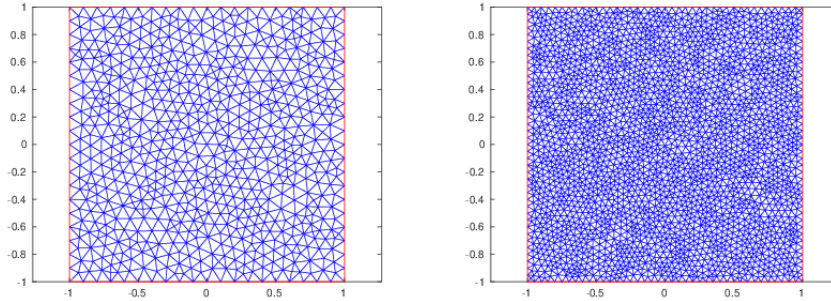


Figure 2: Sequence of unstructured meshes ($h = 0.1$ and 0.05)

We use the unstructured meshes shown in Figure 2 for finite element approximation, giving the high fidelity solutions reported in Figure 3. We have plotted the first six eigenvalues with a legenda and a color code that refers to a local sorting for each value of the parameter. It is clear that the eigenvalues cross each others and that the eigenspaces may have jump discontinuities when a crossing occurs. This phenomenon can be seen, for instance, by looking at the eigenfunctions reported in Figures 4 and 5.

5.1 Reduced order method to obtain λ_1

In order to obtain the first eigenvalue using reduced order method, we consider the snapshot matrix consisting of the first eigenvector u_1 columnwise at sample parameters. In Figure 6

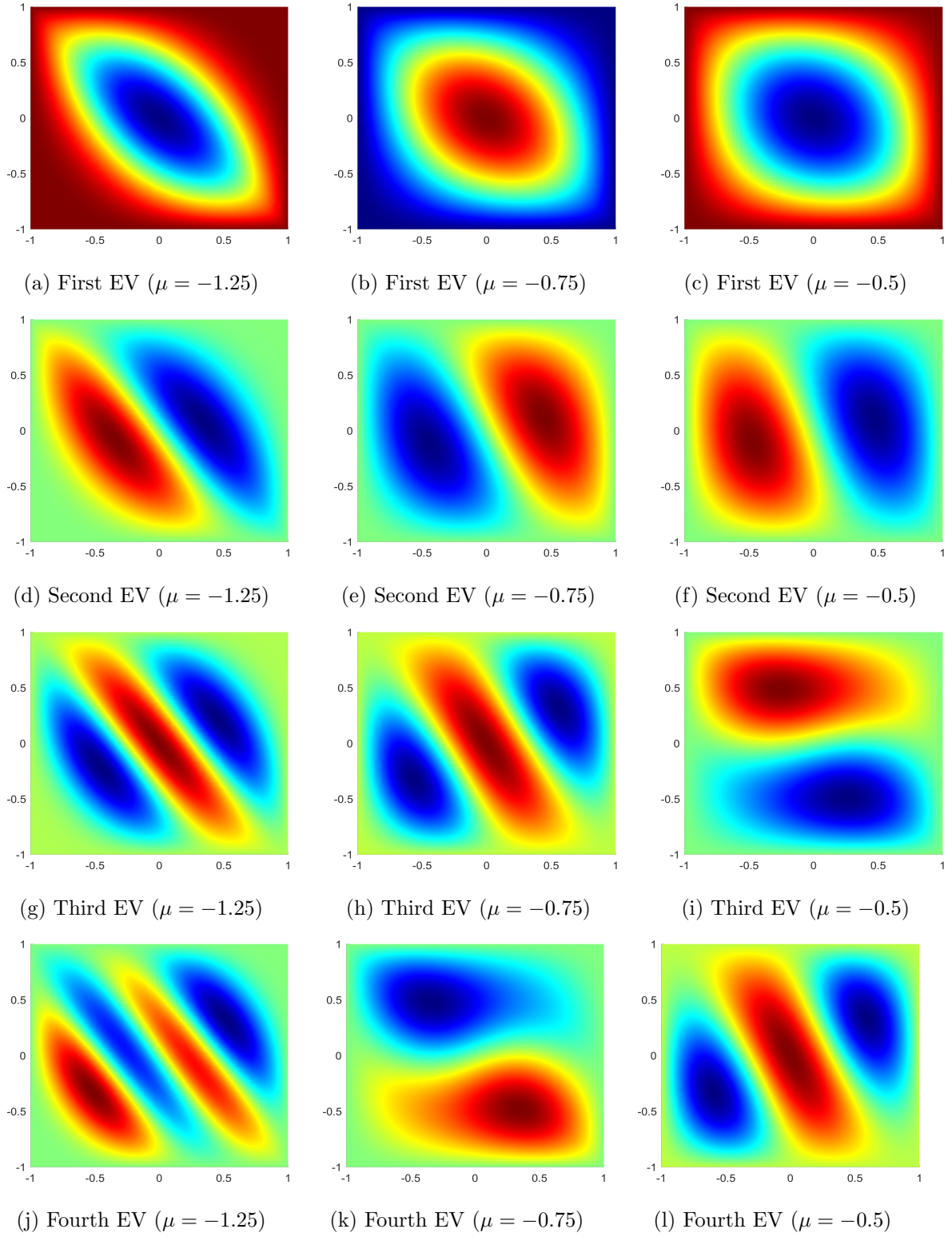


Figure 4: First four eigenvectors at $\mu = -1.25, -0.75, -0.5$ using FEM.

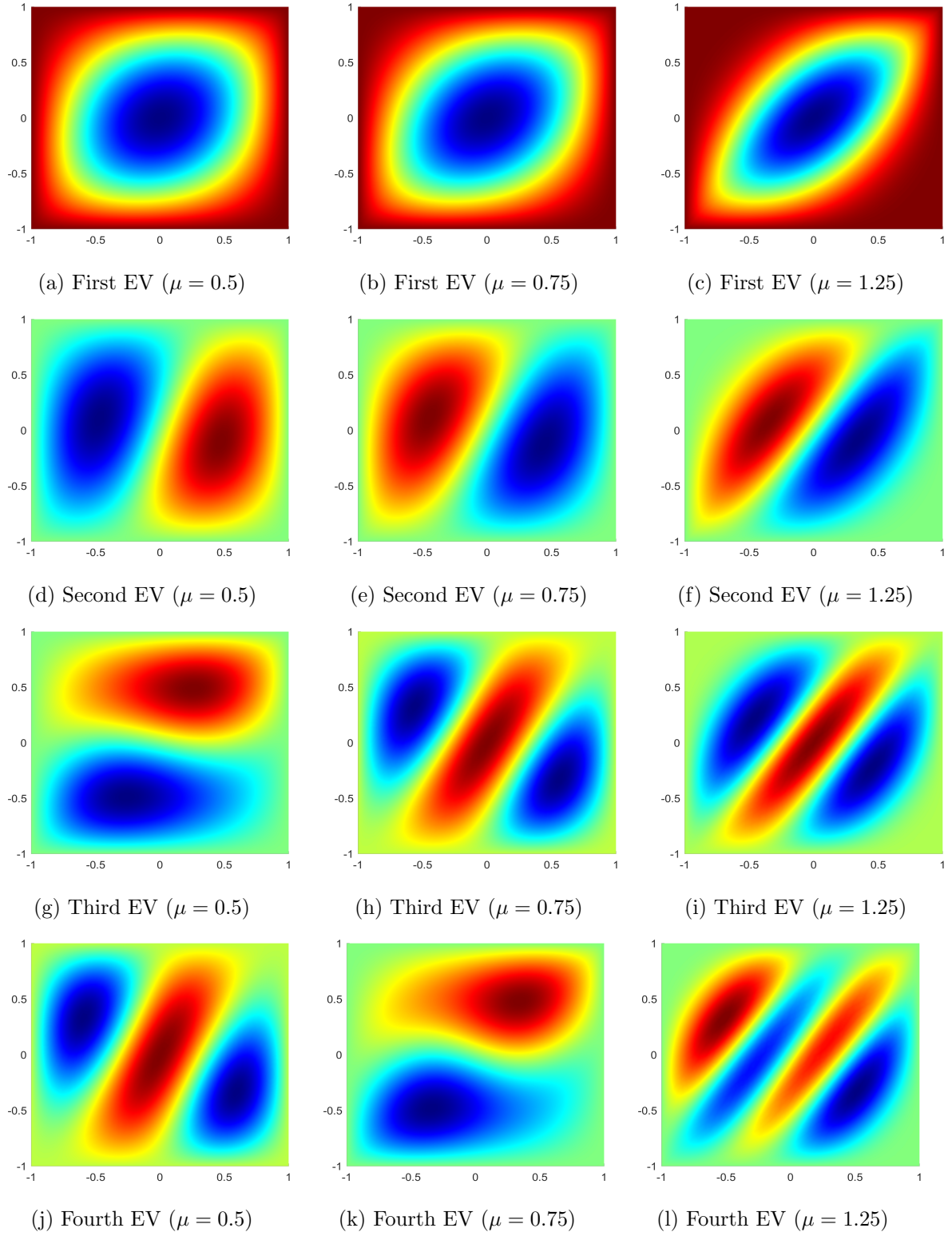


Figure 5: First four eigenfunctions at $\mu = 0.5, 0.75, 1.25$ using FEM

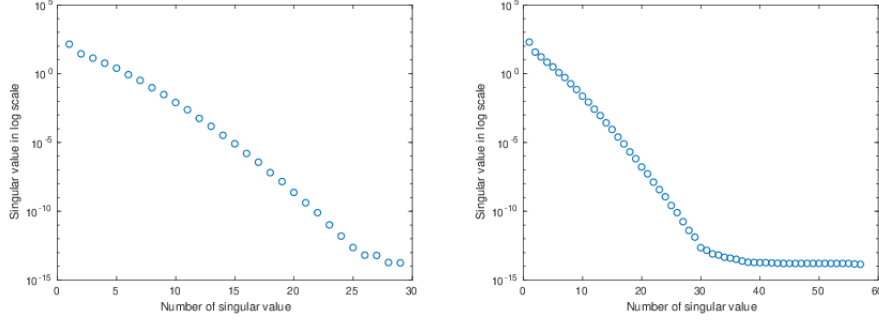


Figure 6: Singular values corresponding to snapshot matrix based on u_1 when $\mu = -1.4 : 0.1 : 1.4$ and $\mu = -1.4 : 0.05 : 1.4$.

we have presented the plot of the singular values of the snapshot matrix for different uniform partitions of the μ interval and observed that the singular values are decaying very fast. In Figure 7 we have shown the plot of first eigenvalue at different number of POD basis functions. It is evident from Figure 7 that the first eigenvalue obtained by ROM is converging to the first eigenvalue of FEM. The first eigenvalues obtained by FEM and ROM and their relative errors at six sample points are reported in Table 1. The ROM dimensions mentioned in Table 1 are obtained using the criterion (3.10) with tolerance 10^{-8} and it can be noted that considering very low ROM dimension, we have achieved an accuracy of order $10^{-7} - 10^{-8}$.

ROM dimension	μ	1st EV(FEM)	1st EV(ROM)	Relative error
9	-1.25	5.98379108	5.98379387	4.7×10^{-7}
	-0.75	7.00305328	7.00305363	5.0×10^{-8}
	-0.50	7.23588322	7.23588390	9.3×10^{-8}
	0.50	7.23585871	7.23585938	9.2×10^{-8}
	0.75	7.00299299	7.00299335	5.1×10^{-8}
	1.25	5.98368037	5.98368313	4.6×10^{-7}
10	-1.25	5.98379108	5.98379164	9.4×10^{-8}
	-0.75	7.00305328	7.00305360	5.8×10^{-8}
	-0.50	7.23588322	7.23588349	3.6×10^{-8}
	0.50	7.23585871	7.23585900	3.9×10^{-8}
	0.75	7.00299299	7.00299332	5.4×10^{-8}
	1.25	5.98368037	5.98368097	1.0×10^{-7}

Table 1: Approximation of λ_1 with snapshot based on u_1 : comparison of FEM and ROM at $h = 0.05$

5.2 Reduced order method to obtain λ_2

In this subsection, we discuss numerical results for the second eigenvalue considering different combinations of eigenvectors in the snapshot matrix.

5.2.1 Results of the EVP considering u_2 in the snapshot matrix

In order to obtain the second eigenvalue using reduced order method, we consider the snapshot matrix consisting of the second eigenvector u_2 columnwise at sample parameters. In Figure 8 we have shown the plot of the first eigenvalue of ROM for different number of POD basis functions.

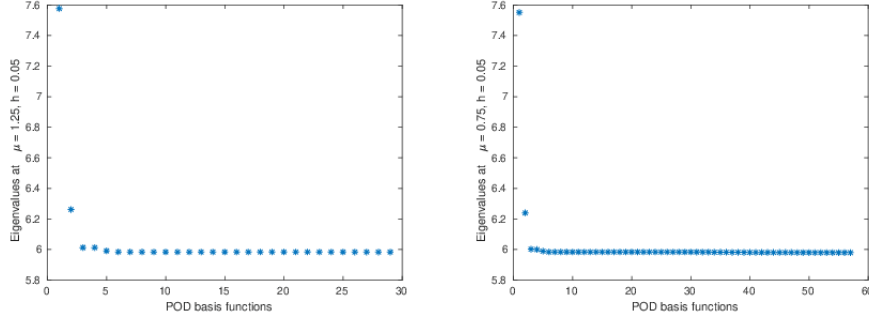


Figure 7: Approximation of λ_1 with snapshot based on u_1 : eigenvalues corresponding to different number of POD basis functions when $\mu = 1.25$ and $h = 0.05$.

It is evident from Figure 8 that the first eigenvalue obtained by ROM is converging to the second eigenvalue of FEM as expected.

The first eigenvalues of ROM, the second eigenvalues of FEM and their relative errors are reported in Table 2. It can be noted that considering very low ROM dimension the relative errors are of order $10^{-7} - 10^{-8}$.

ROM dimension	μ	2nd EV(FEM)	1st EV(ROM)	Relative error
11	-1.25	8.77547249	8.77547548	3.4×10^{-7}
	-0.75	12.86380150	12.86380201	4.0×10^{-8}
	-0.50	13.95750227	13.95750231	3.3×10^{-9}
	0.50	13.95736933	13.95736937	3.2×10^{-9}
	0.75	12.86364140	12.86364192	4.0×10^{-8}
	1.25	8.77689931	8.77690230	3.4×10^{-7}
12	-1.25	8.77547249	8.77547254	4.8×10^{-9}
	-0.75	12.86380150	12.86380156	5.1×10^{-9}
	-0.50	13.95750227	13.95750256	2.0×10^{-8}
	0.50	13.95736933	13.95736962	2.0×10^{-8}
	0.75	12.86364140	12.86364147	5.0×10^{-9}
	1.25	8.77689931	8.77689936	4.9×10^{-9}

Table 2: Approximation of λ_2 with snapshot based on u_2 : comparison of FEM and ROM at $h = 0.05$

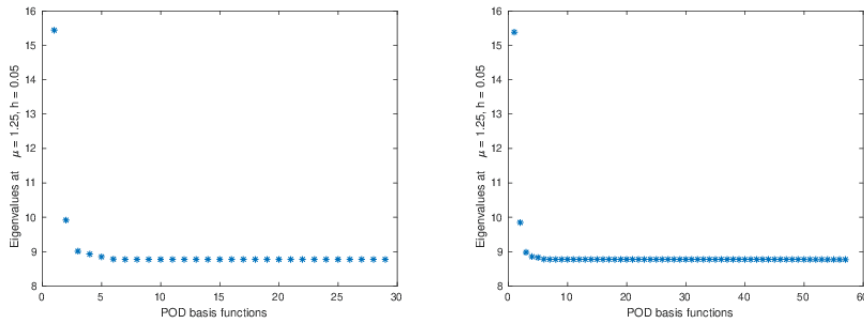


Figure 8: Approximation of λ_2 with snapshot based on u_2 : eigenvalues corresponding to different number of POD basis functions when $\mu = 1.25$ and $h = 0.05$.

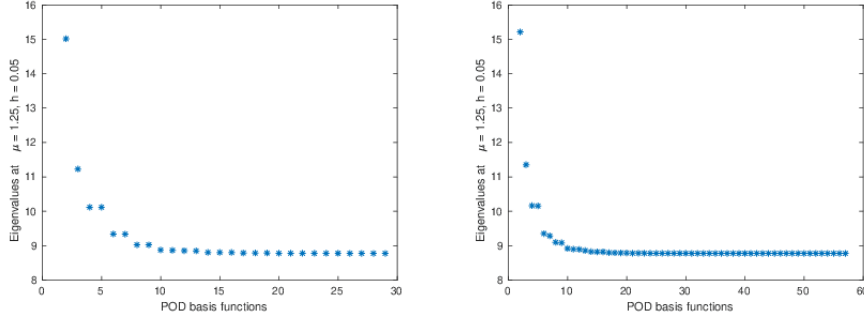


Figure 9: Approximation of λ_2 with snapshot based on $u_1 + u_2$: eigenvalues corresponding to different number of POD basis functions when $\mu = 1.25$ and $h = 0.05$.

ROM dimension	μ	2nd EV(FEM)	2nd EV(ROM)	Relative error
14	-1.25	8.77547249	8.78969339	1.6×10^{-3}
	-0.75	12.86380150	12.86380339	1.4×10^{-7}
	-0.50	13.95750227	13.95750436	1.5×10^{-7}
	0.50	13.95736933	13.95737012	5.6×10^{-8}
	0.75	12.86364140	12.86379512	1.2×10^{-5}
	1.25	8.77689931	8.81325897	4.1×10^{-3}
15	-1.25	8.77547249	8.79049305	1.7×10^{-3}
	-0.75	12.86380150	12.86380446	2.2×10^{-7}
	-0.50	13.95750227	13.95750469	1.7×10^{-7}
	0.50	13.95736933	13.95737042	7.8×10^{-8}
	0.75	12.86364140	12.86390127	2.0×10^{-5}
	1.25	8.77689931	8.82153162	5.0×10^{-3}

Table 3: Approximation of λ_2 with snapshot based on $u_1 + u_2$: comparison of FEM and ROM at $h = 0.05$

5.2.2 Results of the EVP considering $u_1 + u_2$ is in the snapshot matrix

We consider the snapshot matrix consisting of the combination of eigenvectors $u_1 + u_2$ column wise at sample parameters in order to compute the second eigenvalue using the reduced order method. In Figure 9 we have presented the plot of the second eigenvalue of ROM at different number of POD basis functions. The second eigenvalues obtained by FEM and ROM and their relative errors are reported in Table 3.

It can be seen from the Table 2 and Table 3 that considering only u_2 in the snapshot matrix provides us slightly better results than considering $u_1 + u_2$ in the snapshot matrix. However, considering $u_1 + u_2$ in the snapshot matrix, both the eigenvalues λ_1 and λ_2 can be obtained simultaneously.

5.3 Reduced order method to obtain λ_3

In this subsection, we discuss numerical results for the third eigenvalue considering different combinations of eigenvectors in the snapshot matrix. It can be seen from Figure 3 that the third and the fourth eigenvalues are intersecting at some values of μ . We observe many interesting phenomena in this case.

ROM dimension	μ	3rd EV(FEM)	1st EV(ROM)
17	-1.25	12.38270171	12.38271385
	-0.75	21.12292172	15.19805477
	-0.50	22.22010384	15.81534625
	0.50	22.22018744	15.81572205
	0.75	21.12370790	15.19851153
	1.25	12.38958778	12.38960108
18	-1.25	12.38270171	12.38270216
	-0.75	21.12292172	15.31186360
	-0.50	22.22010384	15.92038351
	0.50	22.22018744	15.92406607
	0.75	21.12370790	15.31808566
	1.25	12.38958778	12.38958815

Table 4: Approximation of λ_3 with snapshot based on u_3 at $h = 0.05$

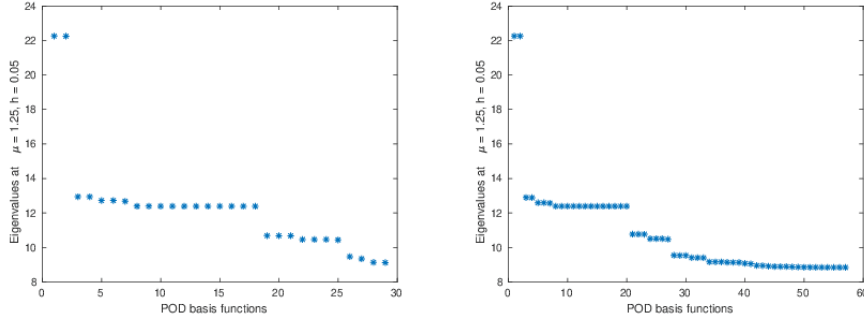


Figure 10: Approximation of λ_3 with snapshot based on u_3 : eigenvalues corresponding to different number of POD basis functions when $\mu = 1.25$ and $h = 0.05$.

5.3.1 Results of the EVP considering only u_3 in the snapshot matrix

Let us consider the snapshot matrix consisting only third eigenvector at the sample points and compute the eigenvalues using reduced order method. Considering the criterion (3.10) with tolerance 10^{-8} , the ROM dimension turns out to be 17 and 18 respectively. In this case, the first eigenvalue of ROM is not matching with the third eigenvalue of FEM, see Table 4. However, when we increase the number of POD basis functions, we notice that the first eigenvalue of the ROM matches with the second eigenvalue of the FEM, whereas the second eigenvalue of the ROM matches with the third eigenvalue of the FEM, see Figure 11. When we consider only the third eigenvector u_3 in the snapshot matrix, we were expecting that the first eigenvalue of the ROM would match with the third eigenvalue of the FEM, but this is not the case. The reason behind this is the fact that the L^2 inner product $(u_2(\mu_i), u_3(\mu_j))$ is not zero for $i \neq j$, so the snapshots contain some component of the second eigenvector. Note that the inner product is zero for $i = j$. In Figure 10 we have presented the plot of first eigenvalue of the ROM at different number of POD basis functions. It can be easily seen from Figure 10 that the first eigenvalue of the ROM is not matching with the third eigenvalue of the FEM. It turns out that the third eigenvector obtained by the ROM is not the same using different number of POD basis functions, see Figure 12.

In Figure 13 we have shown the FEM and ROM eigenvalues for different number of POD basis functions for the parameter space $\mathcal{M} = (-0.6, 0.6)$. Note that for this particular parameter

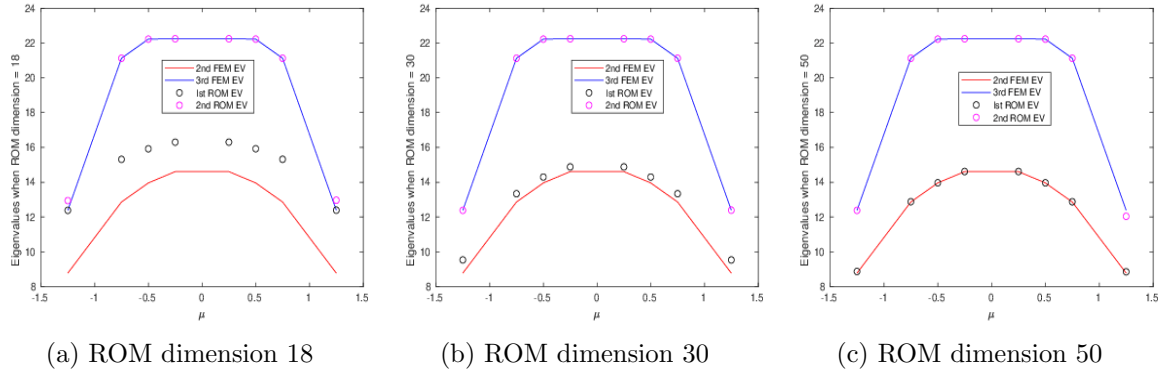


Figure 11: FEM and ROM based eigenvalues at different ROM dimensions

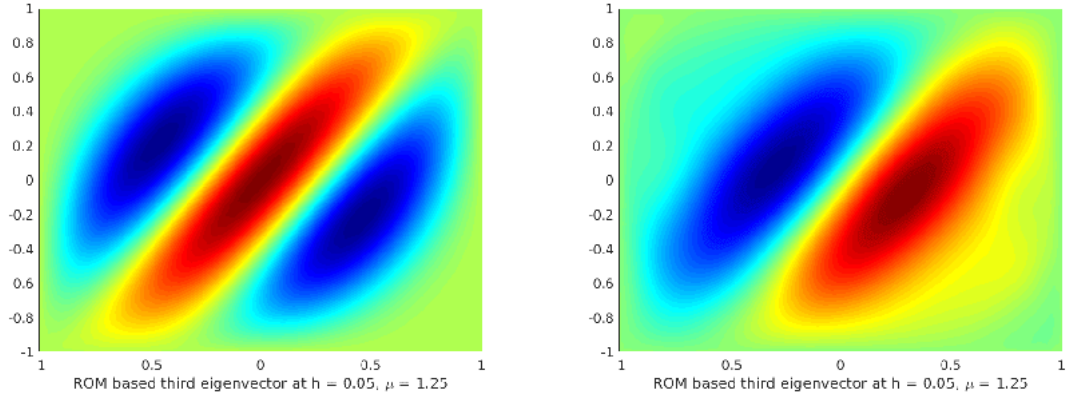


Figure 12: Approximation of u_3 with snapshot based on u_3 when ROM dimension is 18 and 30, $\mu = 1.25$ and $h = 0.05$.

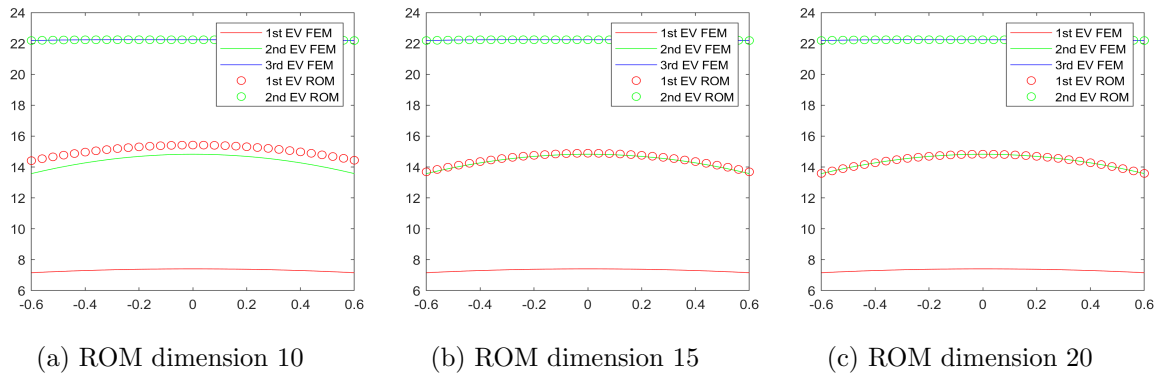


Figure 13: Approximation of eigenvalues with snapshot based on u_3 and $\mathcal{M} = (-0.6, 0.6)$

interval, the two eigenvalues do not intersect (see Figure 3). From the plot one can see that also in this case the situation is not as naively expected: the first eigenvalue of the ROM is matching with the second eigenvalue of the FEM and the second eigenvalue of the ROM is matching with the third eigenvalue of the FEM.

5.3.2 Results of the EVP considering u_3 and u_4 in the snapshot matrix

Since the third and the fourth eigenvalues are intersecting, we consider u_3 and u_4 in the snapshot matrix and compute the eigenvalues using the reduced order method. In Figure 14 we have presented the plot of the first eigenvalue obtained by the ROM. It can be easily seen that the first eigenvalue of ROM is not converging to the third eigenvalue of the FEM. However, the second eigenvalue of the ROM is converging to the third eigenvalue of FEM. In Table 5 we have reported the first and second eigenvalues of the ROM and the third eigenvalue of the FEM.

ROM dimension	μ	3rd EV(FEM)	1st EV(ROM)	2nd EV(ROM)
26	-1.25	12.38270171	10.32768230	12.38271820
	-0.75	21.12292172	14.01748876	21.12292540
	-0.50	22.22010384	14.96276873	22.22010448
	0.50	22.22018744	14.96700836	22.22018808
	0.75	21.12370790	14.02396381	21.12371133
	1.25	12.38958778	10.33922731	12.38960275
30	-1.25	12.38270171	10.35774089	12.38270198
	-0.75	21.12292172	14.02551777	21.12292203
	-0.50	22.22010384	14.96893932	22.22010447
	0.50	22.22018744	14.97067172	22.22018807
	0.75	21.12370790	14.02852884	21.12370817
	1.25	12.38958778	10.36928581	12.38958799

Table 5: Approximation of λ_3 and λ_4 with snapshot based on u_3 and u_4 at $h = 0.05$

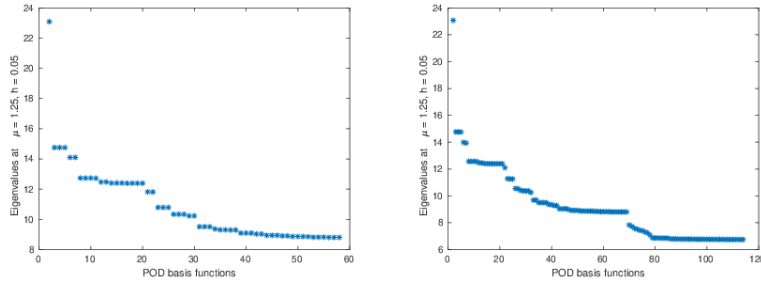


Figure 14: Approximation of λ_3 with snapshot based on u_3 and u_4 : eigenvalues corresponding to different number of POD basis functions when $\mu = 1.25$ and $h = 0.05$.

5.3.3 Results of the EVP considering u_1 , u_2 , and u_3 in the snapshot matrix

Let us consider the snapshot matrix consisting of u_1 , u_2 , and u_3 columnwise at the sample points and compute the first three smallest eigenvalues simultaneously using the reduced order method. Despite the intersection of the third and the fourth eigenvalues, the third eigenvalue of the ROM is converging to the third eigenvalue of the FEM in this case, see Figure 15. In Table 6 we have presented the first, second, and third eigenvalues of ROM at six sample points. It can

ROM dimension.	μ	3rd EV(FEM)	1st EV(ROM)	2nd EV(ROM)	3rd EV(ROM)
32	-1.25	12.38270171	5.98379208	8.77547748	12.38270666
	-0.75	21.12292172	7.00305355	12.86380188	21.12292235
	-0.50	22.22010384	7.23588577	13.95750313	22.22010501
	0.50	22.22018744	7.23586151	13.95737020	22.22018859
	0.75	21.12370790	7.00299337	12.86364179	21.12370853
	1.25	12.38958778	5.98368109	8.77690440	12.38959316
34	-1.25	12.38270171	5.98379248	8.77547319	12.38270251
	-0.75	21.12292172	7.00305409	12.86380239	21.12292251
	-0.50	22.22010384	7.23588378	13.95750246	22.22010682
	0.50	22.22018744	7.23585920	13.95736953	22.22019046
	0.75	21.12370790	7.00299381	12.86364223	21.12370869
	1.25	12.38958778	5.98368176	8.77689991	12.38958860

Table 6: Approximation of λ_1, λ_2 and λ_3 with snapshot based on u_1, u_2 and u_3 at $h = 0.05$

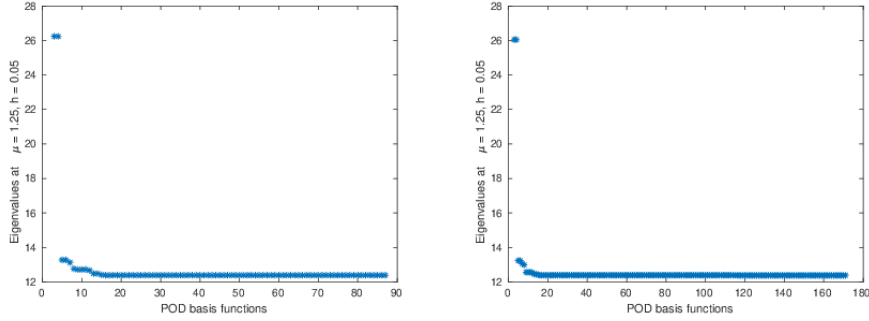


Figure 15: Approximation of λ_3 with snapshot based on u_1, u_2 and u_3 : eigenvalues corresponding to different number of POD basis functions when $\mu = 1.25$ and $h = 0.05$.

be noted that we have obtained the first three smallest eigenvalues simultaneously. Eigenvalues obtained by the ROM are highly accurate. As expected, the third eigenvectors of the ROM are the same even when we increase the number of POD basis functions, see Figure 16.

5.3.4 Results of the EVP considering $u_1 + u_2 + u_3$ in the snapshot matrix

We consider the snapshot matrix consisting $u_1 + u_2 + u_3$ column wise at the sample points and obtain first three smallest eigenvalues simultaneously using reduced order method. In Figure 17 we have shown the plot of third eigenvalues of ROM. It is observed that third eigenvalues of ROM is converging to the third eigenvalue of FEM. In Table 7 we have reported the first, second, and third eigenvalues of ROM at six sample points. We note from Table 7 that first three smallest eigenvalues have been computed simultaneously. As expected, third eigenvectors of ROM are same despite different number of POD basis functions, see Figure 18.

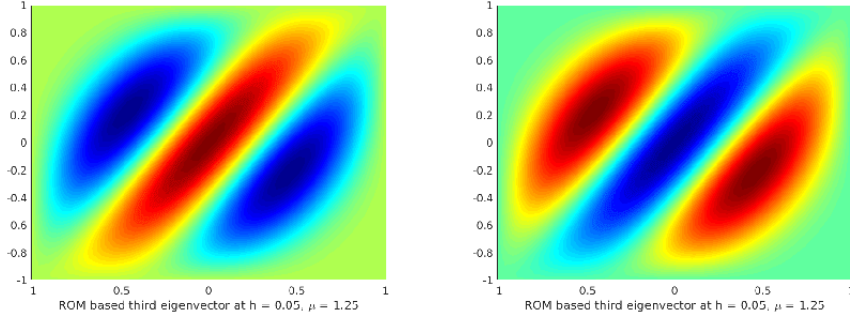


Figure 16: Approximation of u_3 with snapshot based on u_1, u_2 and u_3 when ROM dimension is 34 and 80 respectively ($\mu = 1.25$ and $h = 0.05$.)

ROM dimension	μ	3rd EV(FEM)	1st EV(ROM)	2nd EV(ROM)	3rd EV(ROM)
22	-1.25	12.38270171	5.98859162	8.77898776	12.38307378
	-0.75	21.12292172	7.00306584	12.86381909	21.12293201
	-0.50	22.22010384	7.23591373	13.95751305	22.22012955
	0.50	22.22018744	7.23586309	13.95747389	22.22026978
	0.75	21.12370790	7.00308513	12.86383468	21.12375349
	1.25	12.38958778	5.99388504	8.86730411	12.45479398
25	-1.25	12.38270171	5.98673888	8.77822960	12.38272369
	-0.75	21.12292172	7.00305515	12.86380311	21.12292566
	-0.50	22.22010384	7.23589141	13.95750303	22.22011036
	0.50	22.22018744	7.23586289	13.95738837	22.22019762
	0.75	21.12370790	7.00309327	12.86379347	21.12372327
	1.25	12.38958778	5.99440793	8.79856593	12.40055649

Table 7: Approximation of λ_1, λ_2 and λ_3 with snapshot based on $u_1 + u_2 + u_3$ at $h = 0.05$

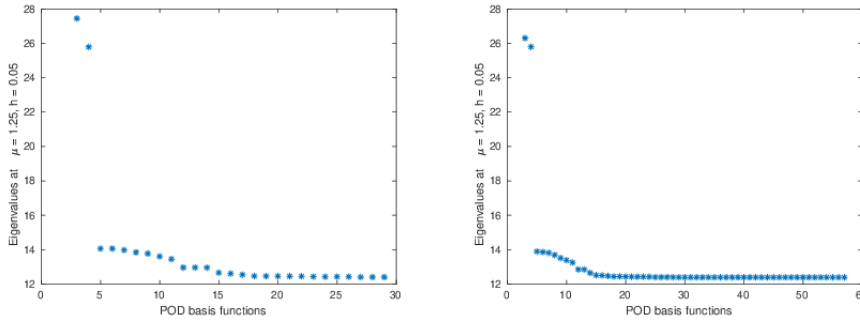


Figure 17: Approximation of λ_3 with snapshot based on $u_1 + u_2 + u_3$: eigenvalues corresponding to different number of POD basis functions when $\mu = 1.25$ and $h = 0.05$.

μ	Relative error (u_1, u_2, u_3)	Relative error ($u_1 + u_2 + u_3$)
-1.25	4.0×10^{-7}	3.0×10^{-5}
-0.75	3.0×10^{-8}	4.8×10^{-7}
-0.50	5.2×10^{-8}	1.2×10^{-6}
0.50	5.2×10^{-8}	3.7×10^{-6}
0.75	3.0×10^{-8}	2.2×10^{-6}
1.25	4.0×10^{-7}	5.2×10^{-3}
-1.25	6.4×10^{-8}	1.8×10^{-6}
-0.75	3.7×10^{-8}	1.9×10^{-7}
-0.50	1.3×10^{-7}	2.9×10^{-7}
0.50	1.4×10^{-7}	4.6×10^{-7}
0.75	3.7×10^{-8}	7.3×10^{-7}
1.25	6.5×10^{-8}	8.8×10^{-4}

Table 8: Relative error between FEM and ROM based third eigenvalue with snapshot based on u_1, u_2, u_3 and $u_1 + u_2 + u_3$ at $h = 0.05$

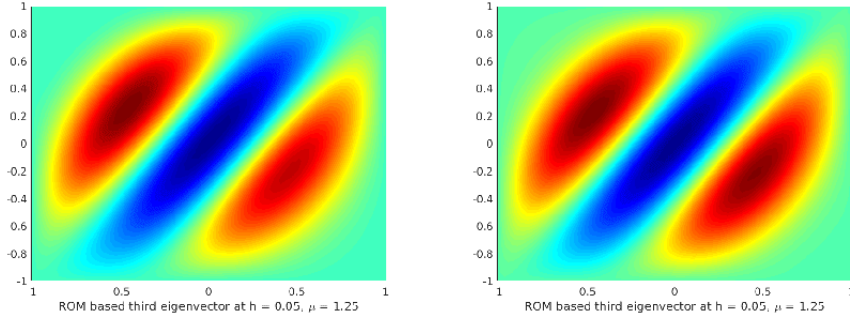


Figure 18: Approximation of u_3 with snapshot based on $u_1 + u_2 + u_3$ when ROM dimension is 37 and 90 respectively ($\mu = 1.25$ and $h = 0.05$).

From Table 8 it is clear that relative error in the case when we considered u_1, u_2 , and u_3 in the snapshot matrix, provides us with slightly better results than when considering $u_1 + u_2 + u_3$. However, the latter case is computationally cheaper.

5.4 Reduced order method to obtain λ_4

In this subsection we discuss numerical results for the fourth eigenvalue considering different combinations of eigenvectors in the snapshot matrix. Since the third and the fourth eigenvalues are intersecting, the numerical results obtained in this subsection present several interesting features.

5.4.1 Results of the EVP considering only u_4 is in the snapshot matrix

Let us consider the snapshot matrix consisting only of the fourth eigenvector u_4 at the sample points and compute the eigenvalues using the reduced order method. In Table 9 the fourth eigenvalue of the FEM and the first eigenvalue of the ROM are reported at few test points. It can be seen that the fourth eigenvalue of the FEM is not matching the first eigenvalue of the ROM, which is also evident from Figure 19. Moreover, when we increase the number of

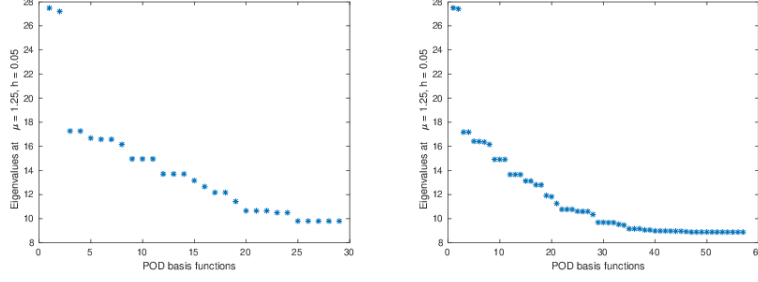


Figure 19: Approximation of λ_4 with snapshot based on u_4 : eigenvalues corresponding to different number of POD basis functions when $\mu = 1.25$ and $h = 0.05$.

ROM dimension	μ	4th EV(FEM)	1st EV(ROM)
20	-1.25	16.13593156	10.63650138
	-0.75	22.08781810	14.31298332
	-0.50	24.02185801	15.23531319
	0.50	24.02234525	15.24102596
	0.75	22.08790319	14.32162342
	1.25	16.13984606	10.65123417
23	-1.25	16.13593156	10.74968666
	-0.75	22.08781810	14.37615778
	-0.50	24.02185801	15.28535039
	0.50	24.02234525	15.28887728
	0.75	22.08790319	14.38179829
	1.25	16.13984606	10.76563540

Table 9: Approximation of λ_4 with snapshot based on u_4 at $h = 0.05$

POD basis functions, we notice that the first eigenvalue of the ROM matches with the second eigenvalues of the FEM, the second eigenvalue of the ROM matches with the third eigenvalue of the FEM, and the third eigenvalues of the ROM matches with the fourth eigenvalues of the FEM, see Figure 20.

5.4.2 Results of the EVP considering u_3 and u_4 in the snapshot matrix

Since λ_3 and λ_4 are intersecting, it is natural to consider both eigenvectors u_3 and u_4 columnwise in the snapshot matrix. In Table 10 we have reported the first and second eigenvalues of the ROM and the fourth eigenvalue of the FEM. As we can see, the second eigenvalue of the ROM matches with the fourth eigenvalues of the FEM. However, as we increase the number of POD basis functions, the second eigenvalue of the ROM is not converging to the fourth eigenvalue of the FEM, see Figure 21.

5.4.3 Results of the EVP considering u_1, u_2, u_3 , and u_4 in the snapshot matrix

Let us consider u_1, u_2, u_3 , and u_4 columnwise in the snapshot matrix and compute the first four smallest eigenvalues simultaneously using the reduced order method. In Figure 22 we have presented the plot of the fourth eigenvalue of the ROM. It can be observed that the fourth eigenvalue of the ROM is converging to the fourth eigenvalue of the FEM. In Table 11 the first four smallest eigenvalues obtained by the ROM and the fourth eigenvalue of the FEM

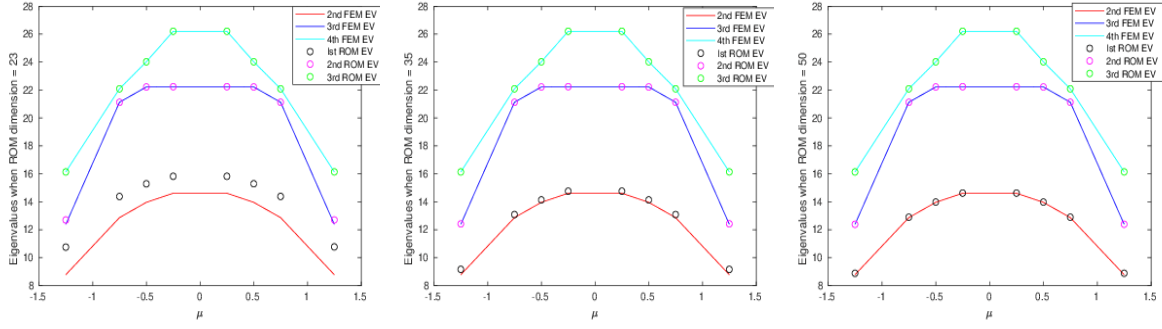


Figure 20: FEM and ROM based eigenvalues at different ROM dimensions

ROM dimension	μ	4th EV(FEM)	1st EV(ROM)	2nd EV(ROM)
26	-1.25	16.13593156	10.32768230	12.38271820
	-0.75	22.08781810	14.01748876	21.12292540
	-0.50	24.02185801	14.96276873	22.22010448
	0.50	24.02234525	14.96700836	22.22018808
	0.75	22.08790319	14.02396381	21.12371133
	1.25	16.13984606	10.33922731	12.38960275
30	-1.25	16.13593156	10.35774089	12.38270198
	-0.75	22.08781810	14.02551777	21.12292203
	-0.50	24.02185801	14.96893932	22.22010447
	0.50	24.02234525	14.97067172	22.22018807
	0.75	22.08790319	14.02852884	21.12370817
	1.25	16.13984606	10.36928581	12.38958799

Table 10: Approximation of λ_3 and λ_4 with snapshot based on u_3 and u_4 at $h = 0.05$

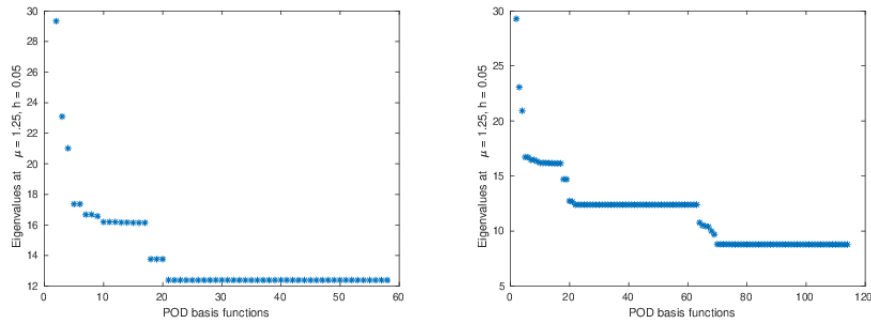


Figure 21: Approximation of λ_4 with snapshot based on u_3 and u_4 : eigenvalues corresponding to different number of POD basis functions when $\mu = 1.25$ and $h = 0.05$.

ROM dim.	μ	4th EV(FEM)	1st EV(ROM)	2nd EV(ROM)	3rd EV(ROM)	4th EV(ROM)
41	-1.25	16.13593156	5.98379230	8.77547626	12.38271182	16.13594735
	-0.75	22.08781810	7.00305433	12.86380238	21.12292388	22.08782059
	-0.50	24.02185801	7.23588570	13.95750374	22.22010425	24.02185908
	0.50	24.02234525	7.23586132	13.95737083	22.22018787	24.02234624
	0.75	22.08790319	7.00299407	12.86364225	21.12370996	22.08790566
	1.25	16.13984606	5.98368138	8.77690306	12.38959840	16.13986166
44	-1.25	16.13593156	5.98379293	8.77547307	12.38270419	16.13593241
	-0.75	22.08781810	7.00305414	12.86380198	21.12292253	22.08781883
	-0.50	24.02185801	7.23588682	13.95750267	22.22010421	24.02185980
	0.50	24.02234525	7.23586277	13.95736973	22.22018781	24.02234706
	0.75	22.08790319	7.00299410	12.86364189	21.12370888	22.08790390
	1.25	16.13984606	5.98368190	8.77689982	12.38959032	16.13984691

Table 11: Approximation of $\lambda_1, \lambda_2, \lambda_3$ and λ_4 with snapshot based on u_1, u_2, u_3 and u_4 at $h = 0.05$

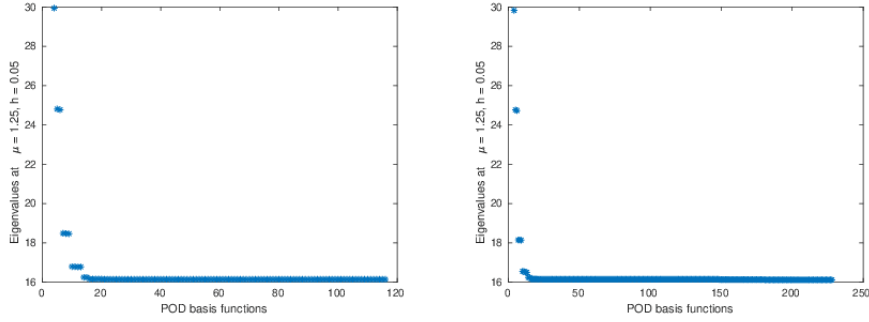


Figure 22: Approximation of λ_4 with snapshot based on u_1, u_2, u_3 and u_4 : eigenvalues corresponding to different number of POD basis functions when $\mu = 1.25$ and $h = 0.05$.

are reported. The obtained numerical results are highly accurate. As expected, the fourth eigenvector of ROM remains the same at different number of POD basis functions, see Figure 23.

5.4.4 Results of the EVP considering $u_1 + u_2 + u_3 + u_4$ in the snapshot matrix

Let us consider the snapshot matrix consisting of the combination $u_1 + u_2 + u_3 + u_4$ columnwise at the sample points and compute the first four smallest eigenvalues simultaneously using the ROM. In Figure 24 we have shown the plot of the fourth eigenvalue of the ROM. It is observed that the fourth eigenvalue of the ROM is converging to the fourth eigenvalue of the FEM even when the number of POD basis functions increases. In Table 12 we have reported the first four smallest eigenvalues of ROM at six sample points. As expected, the fourth eigenvector of the ROM remains the same despite different number of POD basis functions, see Figure 25.

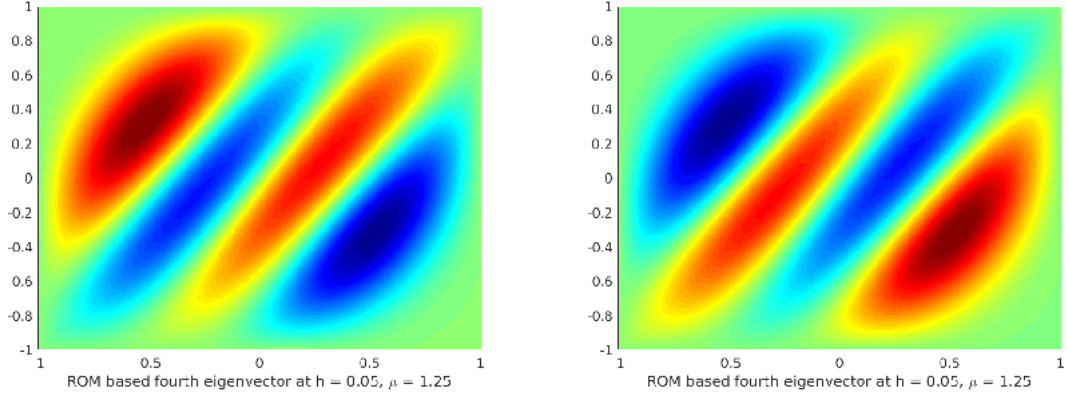


Figure 23: Approximation of u_4 with snapshot based on u_1, u_2, u_3 and u_4 when ROM dimension is 44 and 90 respectively ($\mu = 1.25$ and $h = 0.05$).

ROM dim.	μ	4th EV(FEM)	1st EV(ROM)	2nd EV(ROM)	3rd EV(ROM)	4th EV(ROM)
25	-1.25	16.13593156	6.00975075	8.79767218	12.50952660	16.23425928
	-0.75	22.08781810	7.00397060	12.86485702	21.12369222	22.08841968
	-0.50	24.02185801	7.23599290	13.95753367	22.22012647	24.02187149
	0.50	24.02234525	7.23652419	13.95782932	22.22070774	24.02277614
	0.75	22.08790319	7.00543420	12.86604820	21.12640999	22.09043982
	1.25	16.13984606	6.01170085	8.81168198	12.56293955	16.28632874
28	-1.25	16.13593156	5.99264622	8.78419766	12.51450348	16.24263319
	-0.75	22.08781810	7.00338482	12.86406343	21.12305747	22.08797149
	-0.50	24.02185801	7.23594905	13.95750914	22.22013876	24.02186464
	0.50	24.02234525	7.23637667	13.95781101	22.22063923	24.02275865
	0.75	22.08790319	7.00524937	12.86578107	21.12624130	22.09037931
	1.25	16.13984606	6.01088776	8.80962709	12.52964177	16.27949336

Table 12: Approximation of $\lambda_1, \lambda_2, \lambda_3$ and λ_4 with snapshot based on $u_1 + u_2 + u_3 + u_4$ at $h = 0.05$

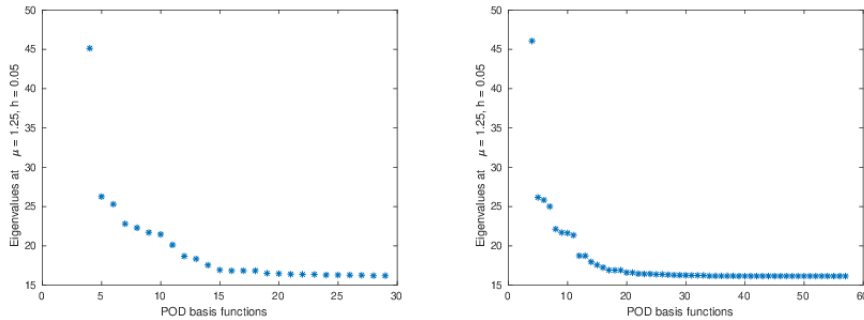


Figure 24: Approximation of λ_4 with snapshot based on $u_1 + u_2 + u_3 + u_4$: eigenvalues corresponding to different number of POD basis functions when $\mu = 1.25$ and $h = 0.05$.

It is apparent from Table 13 that the relative error in the case when we consider u_1, u_2, u_3 , and u_4 in the snapshot matrix is slightly smaller than when considering the combination $u_1 + u_2 + u_3 + u_4$ in the snapshot matrix. However, the latter case is computationally cheaper.

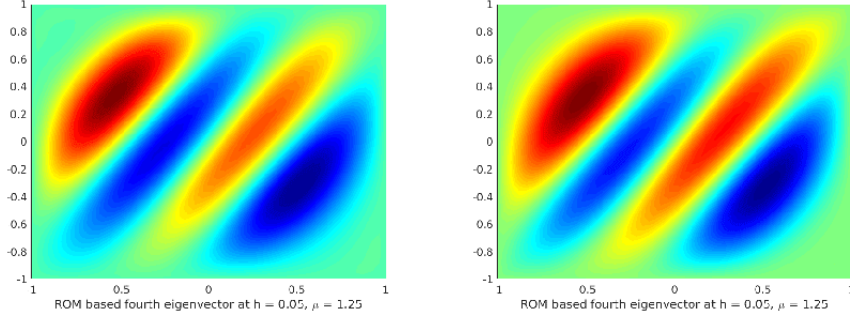


Figure 25: Approximation of u_4 with snapshot based on $u_1 + u_2 + u_3 + u_4$ when ROM dimension is 30 and 50 respectively ($\mu = 1.25$ and $h = 0.05$).

μ	Relative error	Relative error
	u_1, u_2, u_3, u_4	$u_1 + u_2 + u_3 + u_4$
-1.25	9.8×10^{-7}	6.1×10^{-3}
-0.75	1.1×10^{-7}	2.7×10^{-5}
-0.50	4.4×10^{-8}	5.6×10^{-7}
0.50	4.1×10^{-8}	1.8×10^{-5}
0.75	1.1×10^{-7}	1.1×10^{-4}
1.25	9.7×10^{-7}	9.0×10^{-3}
-1.25	5.3×10^{-8}	6.6×10^{-3}
-0.75	3.3×10^{-8}	6.9×10^{-6}
-0.50	7.5×10^{-8}	2.7×10^{-7}
0.50	7.5×10^{-8}	1.7×10^{-5}
0.75	3.2×10^{-8}	1.1×10^{-4}

Table 13: Relative error between FEM and ROM based fourth eigenvalue with snapshot based on u_1, u_2, u_3, u_4 and $u_1 + u_2 + u_3 + u_4$ at $h = 0.05$

6 Numerical results for eigenvalue problem with multiple parameters

In this section we investigate the behavior of the reduced eigenvalues and eigenvectors for different choices of snapshot matrix for the following eigenvalue problem with two parameters:

$$\begin{cases} -\operatorname{div}(A(\boldsymbol{\mu})\nabla u(\boldsymbol{\mu})) = \lambda(\boldsymbol{\mu})u(\boldsymbol{\mu}) & \text{in } \Omega = (0,1)^2 \\ u(\boldsymbol{\mu}) = 0 & \text{on } \partial\Omega \end{cases} \quad (6.1)$$

where the diffusion matrix $A(\boldsymbol{\mu}) \in \mathbb{R}^{2 \times 2}$ is given by

$$A(\boldsymbol{\mu}) = \begin{pmatrix} \frac{1}{\mu_1^2} & \frac{0.7}{\mu_2} \\ \frac{0.7}{\mu_2} & \frac{1}{\mu_2^2} \end{pmatrix},$$

with $\boldsymbol{\mu} = (\mu_1, \mu_2) \in \mathcal{M} \subset \mathbb{R}^2$. The problem is symmetric and the parameter space \mathcal{M} is chosen in such a way that the matrix is positive definite. It can be easily checked that the matrix is positive definite, for instance, for any nonzero value of μ_2 and $\mu_1 \in (-1.42, 1.42) \setminus \{0\}$. For our numerical tests we choose the parameter space to be $\mathcal{M} = [0.4, 1]^2$. In Figure 26 we reported the surface plot for the eigenvalues of the eigenvalue problem (EVP) (26).

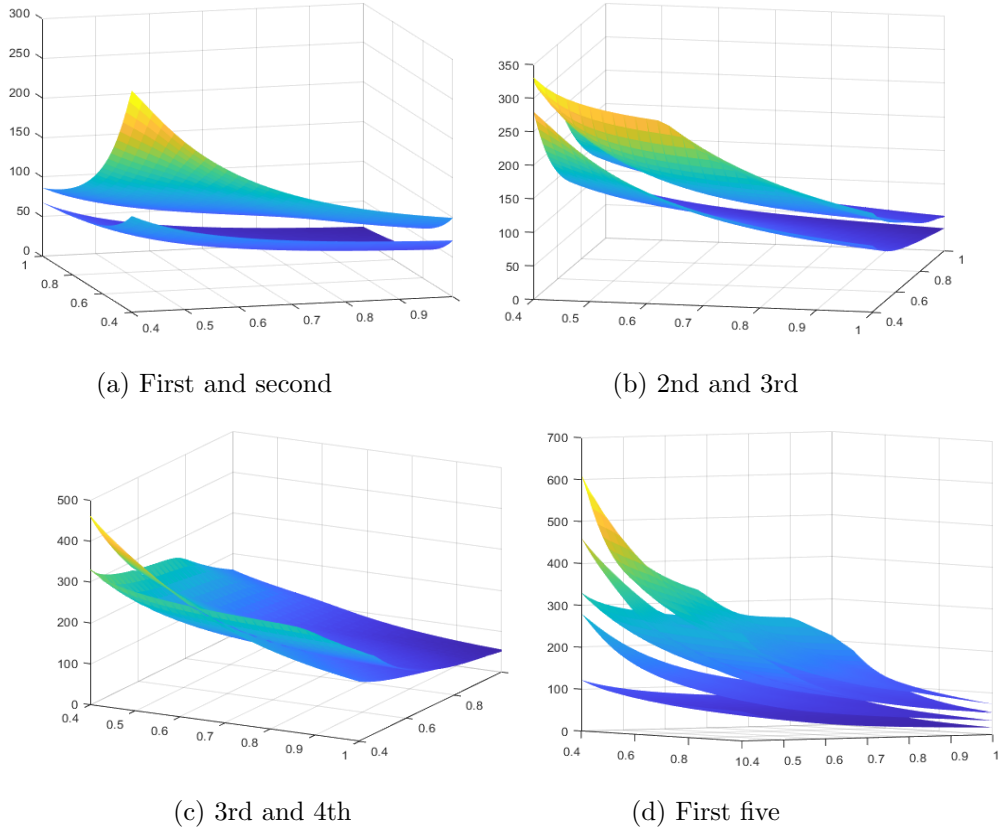


Figure 26: Surface plot for the eigenvalues of the EVP (6.1).

Numerical results with 25 and 49 uniform sample points are presented here. We reported the plot of the singular values of the snapshot matrix, plot for the FOM and the ROM eigenvalues for two sets of parameters, where μ_1 varies and μ_2 is fixed. Also, we have reported the

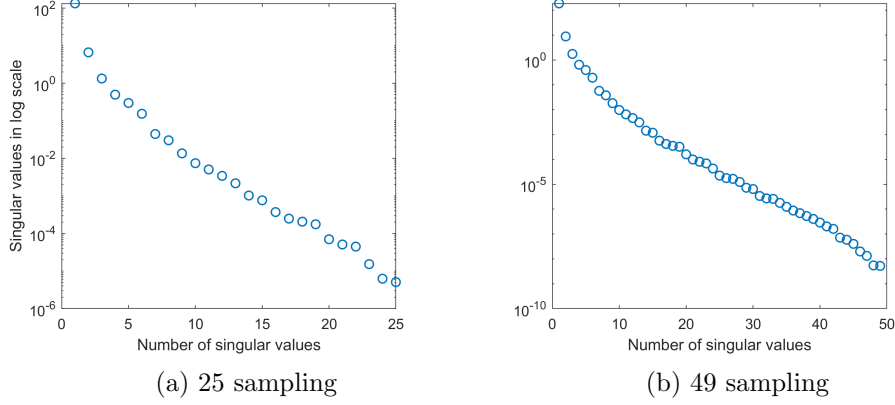


Figure 27: Singular values corresponding to snapshot matrix based on u_1 .

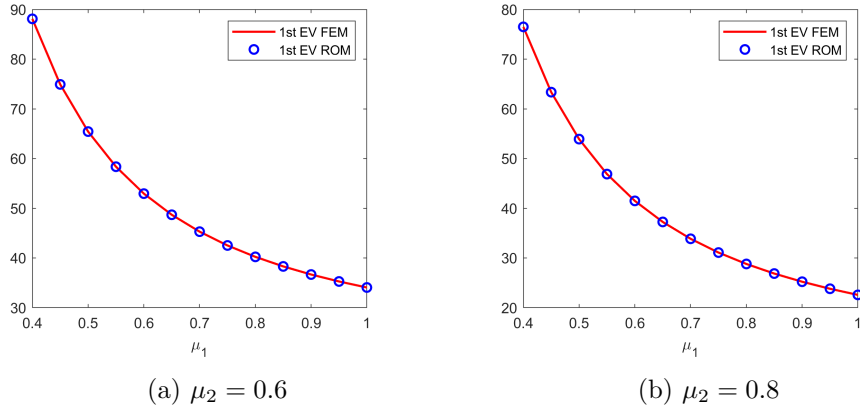


Figure 28: Approximation of λ_1 with snapshot based on u_1 : comparison of FEM and ROM eigenvalues with varying μ_1 and fixed μ_2 , and 49 sample points.

values obtained using the FOM and the ROM at four points $(0.5, 0.6)$, $(0.5, 0.8)$, $(0.8, 0.6)$, and $(0.8, 0.8)$. The number of POD basis is chosen using the criterion (3.10) with tolerance 10^{-8} . To test the behavior of the eigenvalues, we have plotted the eigenvalues of the ROM by varying the number of POD basis at the point $\mu_{1,*} = (0.5, 0.6)$. For all the experiments the mesh size is $h = 0.05$.

6.1 Reduced order method to obtain λ_1

We consider the snapshot matrix consisting of the first eigenvectors column-wise at the sample parameters. In Figure 27 we have shown the plot for the singular values of the snapshot matrix and noticed that the singular values are decaying very fast. As expected, the first eigenvalues of the ROM match with the first eigenvalues of the FOM, which is evident in Figure 28.

The results of FOM and ROM eigenvalues and their relative errors at four sample points are reported in Table 14 for all the sampling. The relative error are of order $10^{-7} - 10^{-9}$. The number of POD dimensions is mentioned in Table 14, which is obtained using the criterion (3.10) with tolerance 10^{-8} . In Figure 29 we have plotted the first eigenvalue at the point $(0.5, 0.6)$ using a different number of POD basis. The eigenvalues are converging to the exact eigenvalue with an increasing number of POD basis.

Sampling points	ROM dim.	μ	1st EV(FEM)	1st EV(ROM)	Rel. Error
25	8	(0.5,0.6)	65.42487472	65.42487526	8.3×10^{-9}
		(0.5,0.8)	53.90654385	53.90654541	2.8×10^{-8}
		(0.8,0.6)	40.22444914	40.22445184	6.7×10^{-8}
		(0.8,0.8)	28.79395153	28.79395783	2.1×10^{-7}
40	9	(0.5,0.6)	65.42487472	65.42487518	7.0×10^{-9}
		(0.5,0.8)	53.90654385	53.90654555	3.1×10^{-8}
		(0.8,0.6)	40.22444914	40.22444771	1.4×10^{-8}
		(0.8,0.8)	28.79395186	28.79395783	1.1×10^{-8}

Table 14: Approximation of λ_1 with snapshot based on u_1 : comparison of FEM and ROM.

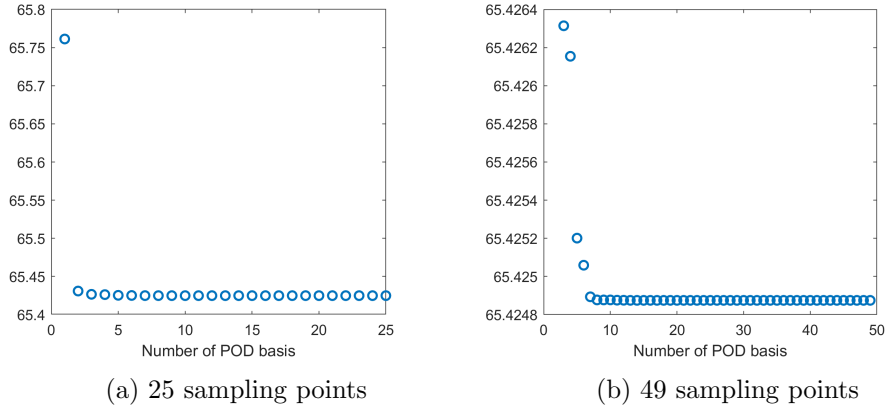


Figure 29: Approximation of λ_1 at $\mu = (0.5, 0.6)$ with snapshot based on u_1 : varying the number of POD basis.

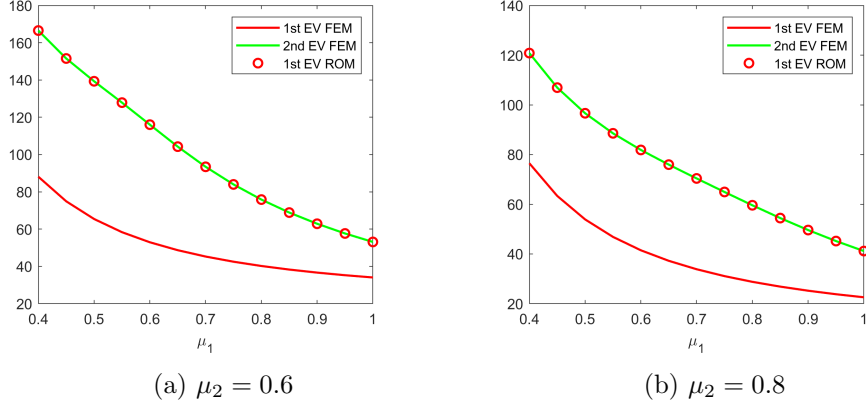


Figure 30: Approximation of λ_2 with snapshot based on u_2 : comparison of FEM and ROM eigenvalues with varying μ_1 and fixed μ_2 , and 49 sample points

Sampling	ROM dim	μ	2nd EV(FEM)	1st EV(ROM)	Rel. Error
25	12	(0.5,0.6)	139.30050529	139.30052177	1.2×10^{-7}
		(0.5,0.8)	96.61215367	96.61216806	1.5×10^{-7}
		(0.8,0.6)	75.84831152	75.84831902	9.8×10^{-8}
		(0.8,0.8)	59.58973796	59.58974344	1.1×10^{-7}
49	12	(0.5,0.6)	139.30050529	139.30051498	6.9×10^{-8}
		(0.5,0.8)	96.61215367	96.61216466	1.1×10^{-7}
		(0.8,0.6)	75.84831152	75.84831665	6.7×10^{-8}
		(0.8,0.8)	59.58973796	59.58974473	9.1×10^{-8}

Table 15: Approximation of λ_2 with snapshot based on u_2 : comparison of FEM and ROM.

6.2 Reduced order method to obtain λ_2

We consider the snapshot matrix consisting of the second eigenvectors columnwise at the sample parameters. As expected, the first eigenvalue of the ROM matches with the second eigenvalue of the FOM, which is evident in Figure 30.

The results of FOM and ROM eigenvalues and their relative errors at four sample points are reported in Table 15 for all the sampling. The relative errors are of order $10^{-7} - 10^{-8}$. The number of POD dimensions is mentioned in Table 15, which is obtained using the criterion (3.10) with tolerance 10^{-8} . In Figure 31 we have plotted the first eigenvalue at the point (0.5, 0.6) using a different number of POD basis. The eigenvalue is converging to the exact eigenvalue with an increasing number of POD basis.

6.3 Reduced order method to obtain λ_3

In this subsection, we discuss the results for third eigenvalues considering different combinations of eigenvectors in the snapshot matrix.

6.3.1 Results of the EVP considering only u_3 in the snapshot matrix

Let us consider the snapshot matrix containing only the third eigenvectors at the sample points. In this case, from Figure 32 it can be seen that the first eigenvalue of the ROM matches the second eigenvalue of the FOM, and the second eigenvalue of the ROM matches the third eigenvalue of the FOM. But, as we consider u_3 in the snapshot matrix, one should expect that

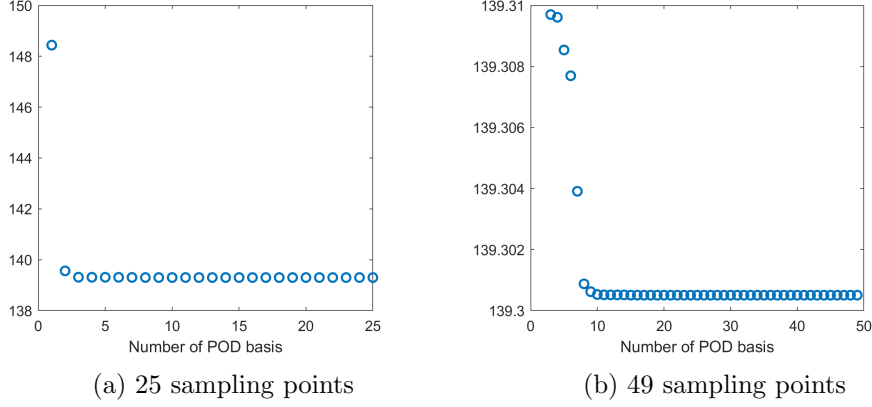


Figure 31: Approximation of λ_2 at $\mu = (0.5, 0.6)$ with snapshot based on u_2 : varying the number of POD basis.

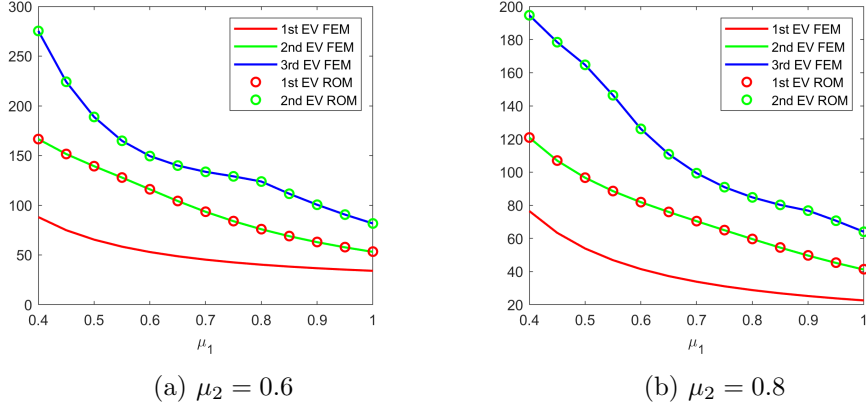


Figure 32: Approximation of λ_3 with snapshot based on u_3 : comparison of FEM and ROM eigenvalues with varying μ_1 and fixed μ_2 , and 49 sample points

the first eigenvalue of the ROM should match with the third eigenvalue of the FOM. The reason behind this is the fact that the L^2 inner product $(u_2(\mu_i), u_3(\mu_j))$ is not zero for $i \neq j$, so the snapshots contain some component of the second eigenvector. If we calculate the inner product $(u_1(\mu_i), u_2(\mu_j))$ then we see that these values are small for $i \neq j$, that is why we are not getting the first eigenvalue. Note that the inner product is zero for $i = j$. From Table 16 it is observed that the maximum relative error among the four test points is 10^{-6} . In Figure 33 we have plotted the second eigenvalue of the ROM at the point $(0.5, 0.6)$ with an increasing number of ROM dimensions. From Figure 33 one can see that if the number of POD basis is up to 38 then the second ROM eigenvalue is converging to the exact one, while then it starts to decrease.

In order to investigate this issue in more detail, we use more sample points and consider all left singular vectors as ROM basis and plot the first four eigenvalues of the FOM and the ROM for $\mu_2 = 0.8$ in Figure 34; we can observe that with the increasing number of sample points all the first four eigenvalues of the ROM converge to the corresponding eigenvalues of the FOM.

6.3.2 Results of the EVP considering u_1 , u_2 , and u_3 in the snapshot matrix

We consider the snapshot matrix containing the first three eigenvectors at the sample points. In this case, all three ROM eigenvalues coincide with the corresponding FOM eigenvalues, as it

Sampling	ROM dim	μ	3rd EV(FEM)	2nd EV(ROM)	Rel. Error
25	21	(0.5,0.6)	188.82589386	188.82716018	6.7×10^{-6}
		(0.5,0.8)	164.71911477	164.71911669	1.1×10^{-8}
		(0.8,0.6)	123.85385935	123.85419564	2.7×10^{-6}
		(0.8,0.8)	84.76248191	84.76248514	3.8×10^{-8}
49	24	(0.5,0.6)	188.82589386	188.82590770	7.3×10^{-8}
		(0.5,0.8)	164.71911477	164.71911878	2.4×10^{-8}
		(0.8,0.6)	123.85385935	123.85387416	1.1×10^{-7}
		(0.8,0.8)	84.76248191	84.76248574	4.5×10^{-8}

Table 16: Approximation of λ_3 with snapshot based on u_3 : comparison of FEM and ROM.

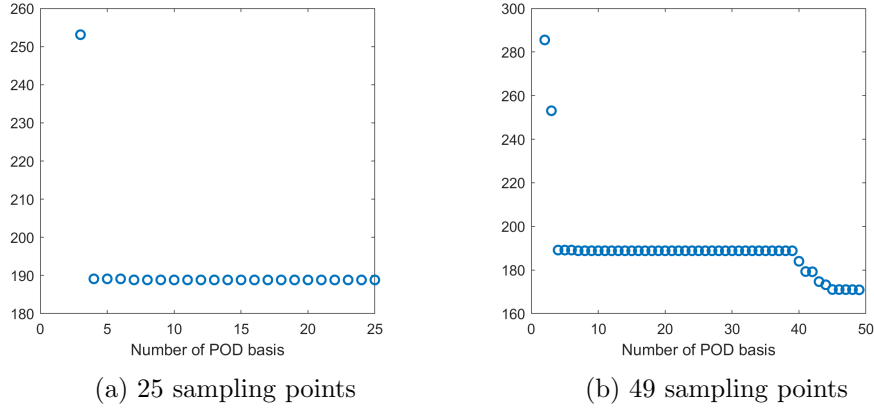


Figure 33: Approximation of λ_3 at $\mu = (0.5, 0.6)$ with snapshot based on u_3 : varying the number of POD basis.

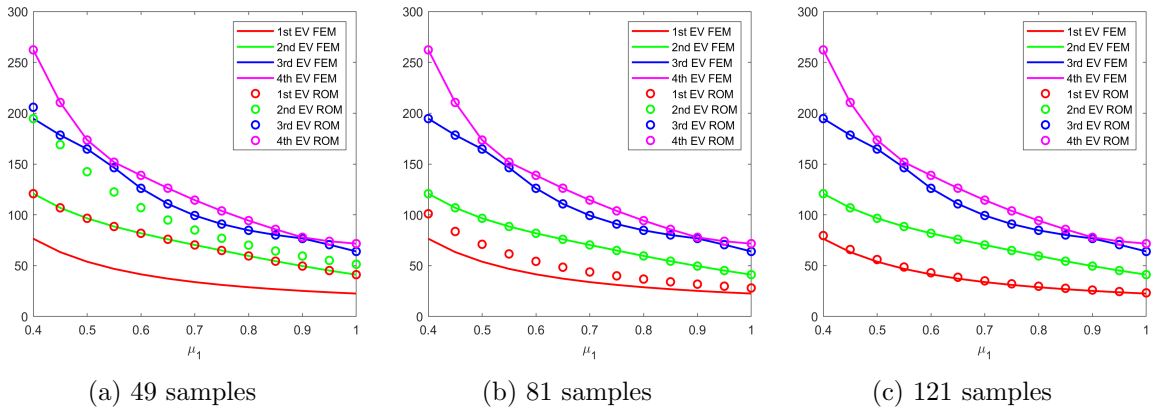


Figure 34: Approximation of λ_3 with snapshot based on u_3 : comparison of FEM and ROM eigenvalues with varying μ_1 and $\mu_2 = 0.8$, and with different number of sample points

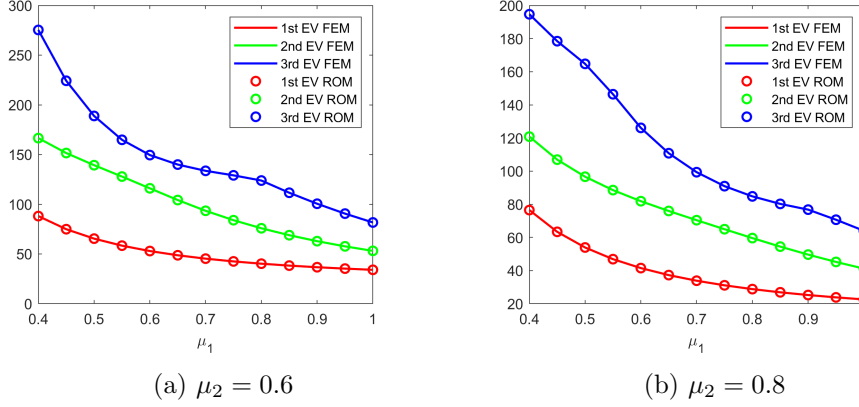


Figure 35: Approximation of λ_3 with snapshot based on u_1, u_2, u_3 : comparison of FEM and ROM eigenvalues with varying μ_1 and fixed μ_2 , and 49 sample points.

Sampling	dim ROM	μ	3rd EV(FEM)	3rd EV(ROM)	Rel. Error (λ_3)
25	32	(0.5,0.6)	188.82589386	188.82590469	5.7×10^{-8}
		(0.5,0.8)	164.71911477	164.71917647	3.7×10^{-7}
		(0.8,0.6)	123.85385935	123.85438852	4.2×10^{-6}
		(0.8,0.8)	84.76248191	84.76249669	1.7×10^{-7}
45	33	(0.5,0.6)	188.82589386	188.82591285	1.0×10^{-7}
		(0.5,0.8)	164.71911477	164.71913934	1.4×10^{-7}
		(0.8,0.6)	123.85385935	123.85389384	2.7×10^{-7}
		(0.8,0.8)	84.76248191	84.76249350	1.3×10^{-7}

Table 17: Approximation of λ_3 with snapshot based on u_1, u_2, u_3 : comparison of FEM and ROM.

can be seen in Figure 35.

The eigenvalues of the FOM and the ROM at the four sample points are reported in Table 17. The relative error between the FOM and ROM eigenvalues are also reported and the maximum error is 10^{-6} . Even if we are increasing the number of POD basis then also the 3rd eigenvalue corresponding to the ROM converges to the 3rd eigenvalue of the FOM as it is shown in Figure 36.

6.3.3 Results of the EVP considering $u_1 + u_2 + u_3$ in the snapshot matrix

The results of the ROM are good when we consider the first three eigenvectors in the snapshot matrix and the order of the eigenvalues is also preserved. However, the number of snapshots is three times the number of sample points. In order to try to reduce the computational cost, we consider the snapshot matrix containing the sum of the first three eigenvectors at the sample points as the column. Then the number of columns of the snapshot matrix is equal to the number of snapshots and the snapshots contain some components of all three eigenvectors. In this case, also, the first three eigenvalues of the ROM coincide with the first eigenvalues of the FOM and preserve the order, see Figure 37.

The 3rd eigenvalues of the ROM and the FOM at the four test points and the corresponding relative errors are reported in Table 18. The maximum relative error is 10^{-4} . Note that by taking the combination of the eigenvectors we reduce the number of snapshots at the price of having results which are not as good as in the former case when we considered all three

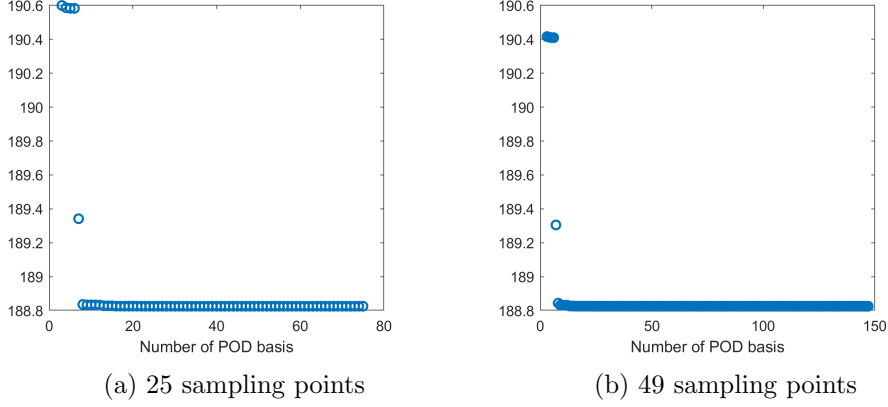


Figure 36: Approximation of λ_3 at $\mu = (0.5, 0.6)$ with snapshot based on u_1, u_2, u_3 : varying the number of POD basis.

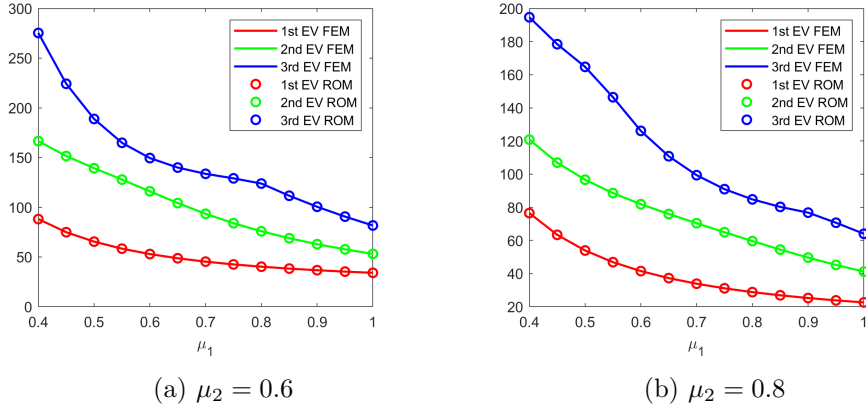


Figure 37: Approximation of $\lambda_1, \lambda_2, \lambda_3$ with snapshot based on $u_1 + u_2 + u_3$: comparison of FEM and ROM eigenvalues with varying μ_1 and fixed μ_2 , and 49 sample points.

eigenvectors. In Figure 39 we reported the third eigenvectors obtained using the FOM and the ROM at the four sample points and they are matching up to the sign.

6.4 Reduced order method to obtain λ_4

In this subsection we will find the fourth eigenvalue of the problem using different choices of snapshot matrix.

6.4.1 Results of the EVP considering only u_4 in the snapshot matrix

First, we consider the snapshot matrix containing only the fourth eigenvector at the sample points. In Figure 40 we have shown the first four eigenvalues of the FOM and the first three eigenvalues of the ROM for the parameters μ_1 ranging from 0.4 to 1 with step 0.05 and μ_2 equal to 0.6 and 0.8 respectively. In this case, the fourth eigenvalue of the FOM model is not matching with the first eigenvalue of the ROM, nor with the second eigenvalue of the ROM, but with the third eigenvalue of the ROM. This is consequence of the fact that the inner products $(u_2(\mu_i), u_4(\mu_j))$ and $(u_3(\mu_i), u_4(\mu_j))$, for $i \neq j$, are not zero nor small. The first eigenvalue of the ROM coincides with the second eigenvalue of the FOM, the second eigenvalue of the

Sampling	ROM dim	μ	3rd EV(FEM)	3rd EV(ROM)	Rel. Error(λ_3)
25	22	(0.5,0.6)	188.82589386	188.82837895	1.3×10^{-5}
		(0.5,0.8)	164.71911477	164.72021897	6.7×10^{-6}
		(0.8,0.6)	123.85385935	123.87322460	1.5×10^{-4}
		(0.8,0.8)	84.76248191	84.76361731	1.3×10^{-5}
49	28	(0.5,0.6)	188.82589386	188.82593692	2.2×10^{-7}
		(0.5,0.8)	164.71911477	164.71919081	4.6×10^{-7}
		(0.8,0.6)	123.85385935	123.85406453	1.6×10^{-6}
		(0.8,0.8)	84.76248191	84.76249965	2.0×10^{-7}

Table 18: Approximation of λ_3 with snapshot based on $u_1 + u_2 + u_3$: comparison of FEM and ROM.

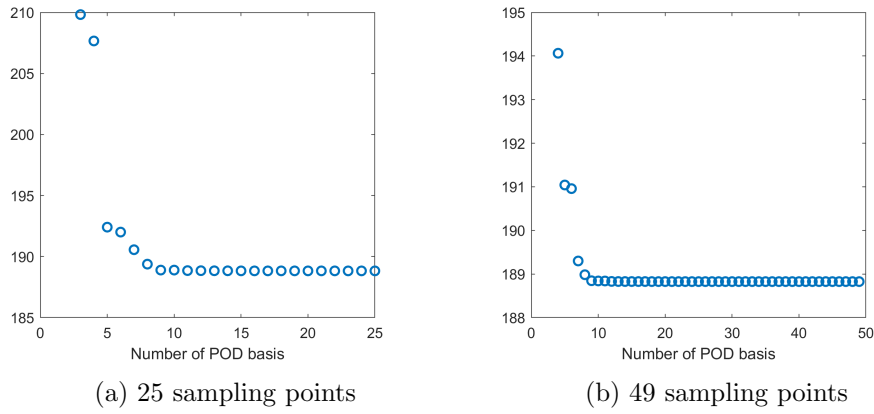


Figure 38: Approximation of λ_3 at $\mu = (0.5, 0.6)$ with snapshot based on $u_1 + u_2 + u_3$: varying the number of POD basis.

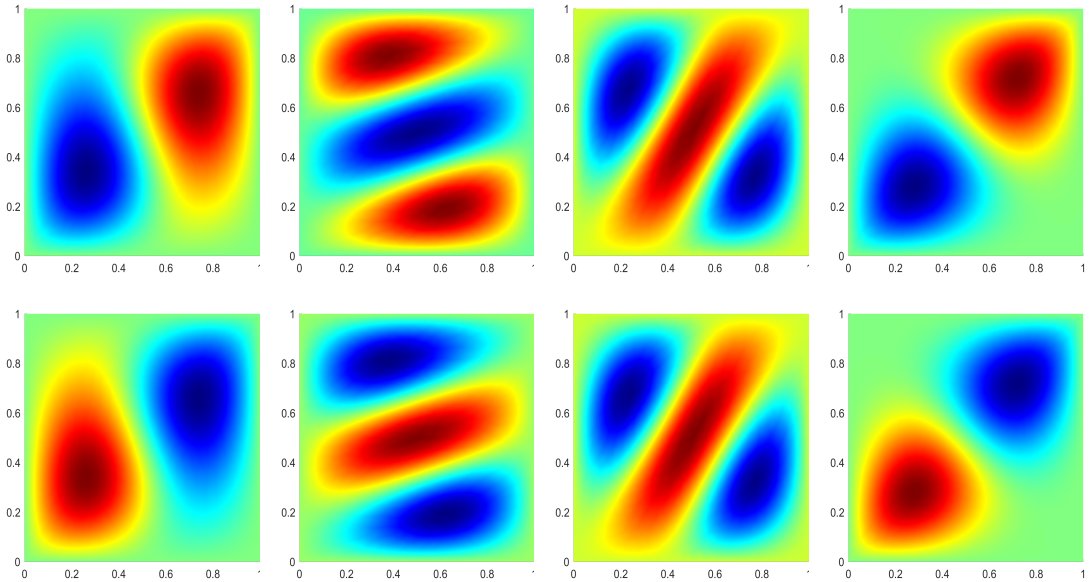


Figure 39: Comparison of 3rd eigenvectors using FEM (1st row) and ROM (2nd row) with snapshot based on $u_1 + u_2 + u_3$ at four points.

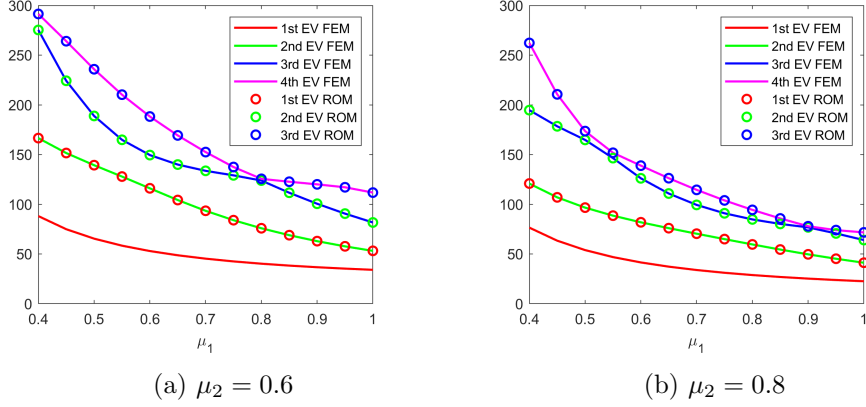


Figure 40: Approximation of λ_4 with snapshot based on u_4 : comparison of FEM and ROM eigenvalues with varying μ_1 and fixed μ_2 , and 49 sample points.

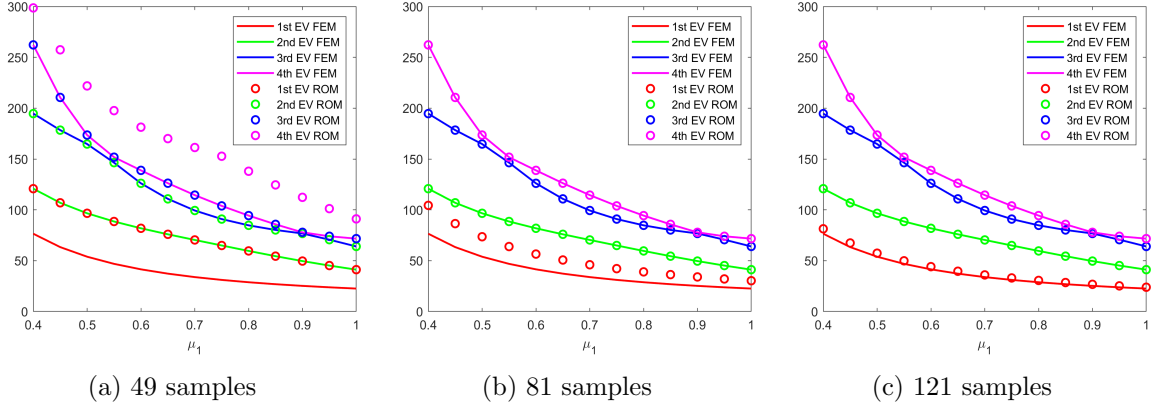


Figure 41: Approximation of $\lambda_1, \lambda_2, \lambda_3, \lambda_4$ with snapshot based on u_4 : comparison of FEM and ROM eigenvalues with varying μ_1 and $\mu_2 = 0.8$, and with different number of sample points.

ROM coincides with the third eigenvalue of the FOM, and the third eigenvalue of the ROM coincides with the fourth eigenvalue of the FOM. In Figure 41 we have shown the eigenvalues of the FOM and the ROM with different number of sample points when we consider all the left singular vectors as a basis. We can see that as we increase the number of sample points the first eigenvalue of the ROM converges to the first eigenvalue of the FOM. Thus all four ROM eigenvalues follow the order of the FOM.

The fourth eigenvalue of the FOM and the corresponding ROM at the four test points are presented and the relative errors are presented in Table 19. The dimension of the reduced system obtained using the criterion (3.10) is also mentioned in the same table. The maximum relative error among the four test points is 10^{-6} . Note that when we increase the number of sample points then the results are improving. We have shown the plot for the ROM at the point (0.5, 0.6) with the different ROM dimensions in Figure 42 and one can see that the ROM eigenvalue is converging to the exact eigenvalue when the ROM dimension is more than 4.

6.4.2 Results of the EVP considering u_3 and u_4 in the snapshot matrix

Since the third and fourth eigenvectors are intersecting, let us put u_3 and u_4 in the snapshot matrix and observe the result. Now the results behave as in the case when we considered only

Sampling	ROM dim	μ	4th EV(FEM)	3rd EV(ROM)	Rel. Error
25	22	(0.5,0.6)	235.80616993	235.80648771	1.3×10^{-6}
		(0.5,0.8)	173.56836538	173.56839422	1.6×10^{-7}
		(0.8,0.6)	125.56104288	125.56186825	6.5×10^{-6}
		(0.8,0.8)	94.35030619	94.35031462	8.9×10^{-8}
49	28	(0.5,0.6)	235.80616993	235.80617183	8.0×10^{-9}
		(0.5,0.8)	173.56836538	173.56838071	8.8×10^{-8}
		(0.8,0.6)	125.56104288	125.56105296	8.0×10^{-8}
		(0.8,0.8)	94.35030619	94.35030733	1.2×10^{-8}

Table 19: Approximation of λ_4 with snapshot based on u_4 : comparison of FEM and ROM.

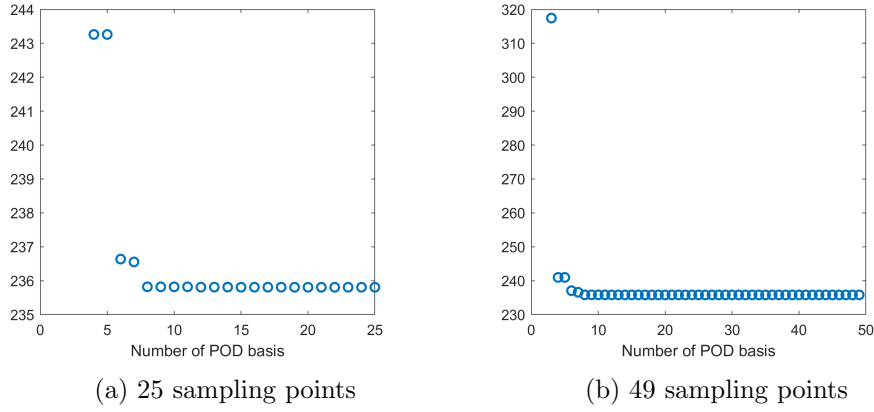


Figure 42: Approximation of λ_4 at $\mu = (0.5, 0.6)$ with snapshot based on u_4 : varying the number of POD basis.

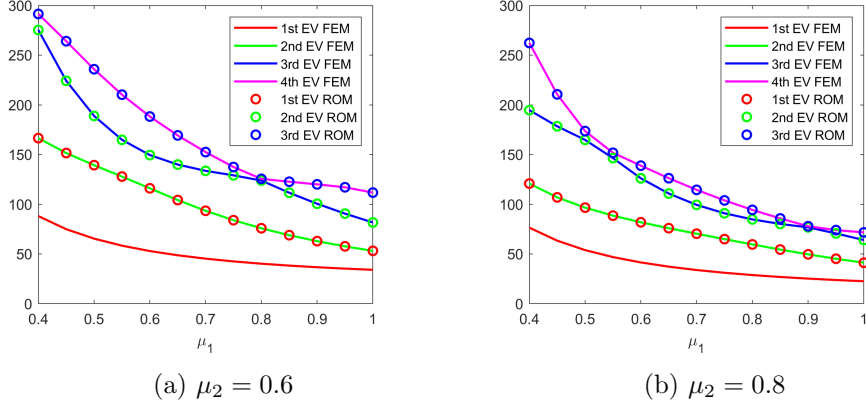


Figure 43: Approximation of eigenvalues with snapshot based on u_3 and u_4 : comparison of FEM and ROM eigenvalues with varying μ_1 and fixed μ_2 , and 49 sample points.

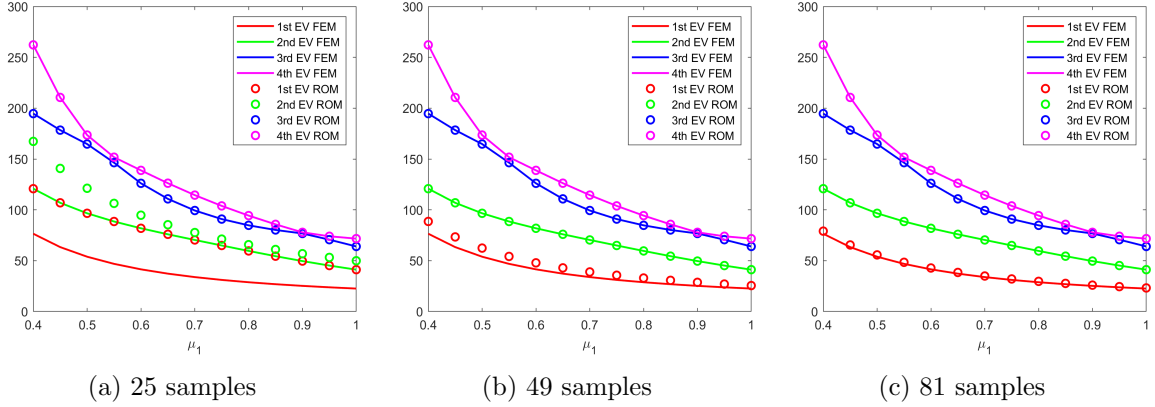


Figure 44: Approximation of eigenvalues with snapshot based on u_3 and u_4 : comparison of FEM and ROM eigenvalues with varying μ_1 and $\mu_2 = 0.8$, and with different number of sample points.

u_4 in the snapshot matrix, that is the fourth eigenvalue of the FOM matches with the third eigenvalue of the ROM and so on, see Figure 43). In Figure 44 we have shown the eigenvalues of the FOM and the ROM with different number of sample points and consider all the left singular vectors of the snapshot matrix as a basis. We can see that as we increase the number of sample points the first eigenvalue of the ROM converges to the first eigenvalue of the FOM. Thus all four ROM eigenvalues follow the order of the FOM. The fourth eigenvalue of the FOM and the corresponding ROM at the four test points are presented in Table 20 and the maximum relative error is 10^{-7} .

6.4.3 Results of the EVP considering u_1 , u_2 , u_3 , and u_4 in the snapshot matrix

Then we consider the snapshot matrix containing the first fourth eigenvectors at the sample points. The first four eigenvalues of the FOM and ROM are plotted in Figure 46 for the parameters μ_1 ranging from 0.4 to 1 with step 0.05 and μ_2 equal to 0.6 and 0.8, respectively. In this case, all the first four eigenvalues of the ROM match with the first four eigenvalues of the FOM. In this case, considering all the left singular vectors of the snapshot matrix as a basis, the eigenvalues are stable (see Figure 47).

Sampling	ROM dim	μ	4th EV(FEM)	3rd EV(ROM)	Rel. Error
25	30	(0.5,0.6)	235.80616993	235.80618623	6.9×10^{-8}
		(0.5,0.8)	173.56836538	173.56838092	8.9×10^{-8}
		(0.8,0.6)	125.56104288	125.56105844	1.2×10^{-7}
		(0.8,0.8)	94.35030619	94.35030784	1.7×10^{-8}
49	31	(0.5,0.6)	235.80616993	235.80617885	3.7×10^{-8}
		(0.5,0.8)	173.56836538	173.56838605	1.1×10^{-7}
		(0.8,0.6)	125.56104288	125.56105806	1.2×10^{-7}
		(0.8,0.8)	94.35030619	94.35030780	1.7×10^{-8}

Table 20: Approximation of λ_4 with snapshot based on u_3, u_4 : comparison of FEM and ROM.

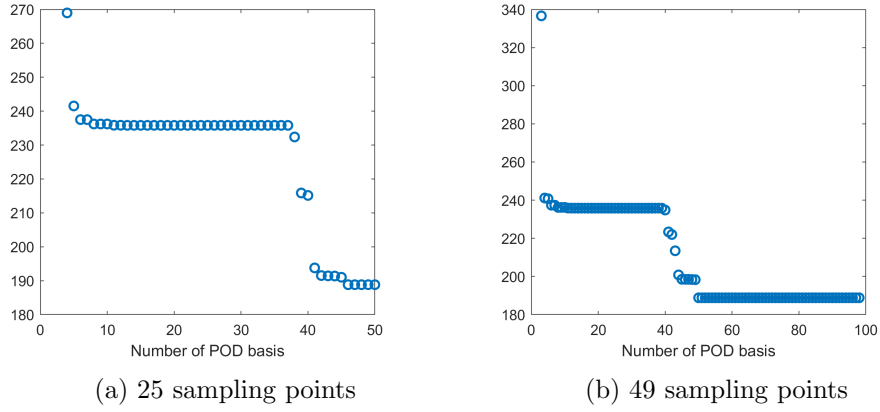


Figure 45: Approximation of λ_4 at $\mu = (0.5, 0.6)$ with snapshot based on u_3, u_4 : varying the number of POD basis.

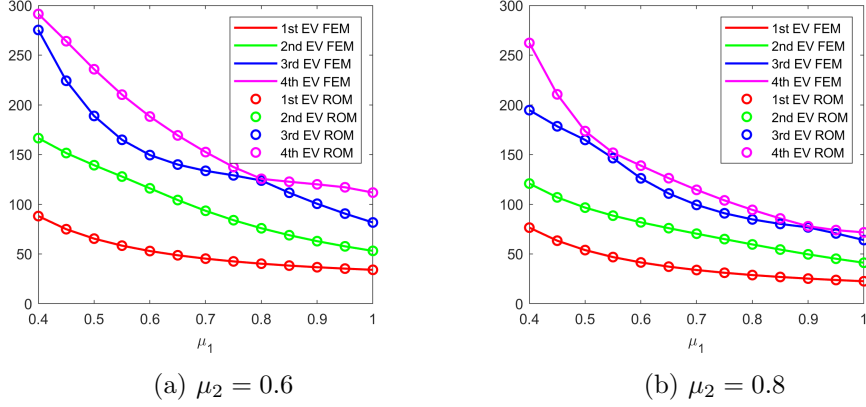


Figure 46: Approximation of eigenvalues with snapshot based on u_1, u_2, u_3 , and u_4 : comparison of FEM and ROM eigenvalues with varying μ_1 and fixed μ_2 , and 49 sample points.

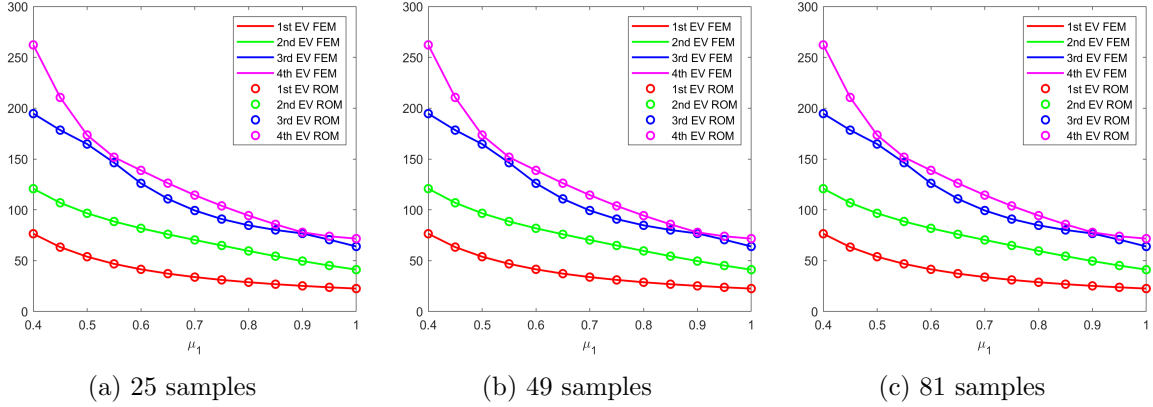


Figure 47: Approximation of eigenvalues with snapshot based on u_1, u_2, u_3 , and u_4 : comparison of FEM and ROM eigenvalues with varying μ_1 and $\mu_2 = 0.8$ for different sample points.

The fourth eigenvalue of the FOM and the fourth eigenvalue of the ROM at the four test points and their relative errors are presented in Table 21. The dimension of the reduced system obtained using the criterion (3.10) is also mentioned in the same table. The maximum relative error among the four test points is 10^{-7} . We have shown the plot for the fourth eigenvalue of the ROM at the point (0.5, 0.6) with the different ROM dimensions in Figure 48 and one can see that the ROM eigenvalue is converging to the exact eigenvalue when the ROM dimension is more than 15.

6.4.4 Results of the EVP considering $u_1 + u_2 + u_3 + u_4$ in the snapshot matrix

The results corresponding to the case when we consider all the first four eigenvectors in the snapshot matrix are good and the order of the eigenvalues of the ROM and the FOM are the same, but the number of snapshots is four times than the sample points. In order to reduce the computational cost, we add the first four eigenvectors and choose the resulting vector as a snapshot to control the number of snapshots. Also in this case all the ROM eigenvalues match the corresponding FOM eigenvalues, as it is shown in Figure 49.

The fourth eigenvalue of the FOM and the fourth eigenvalue of the ROM at the four test points and their relative errors are presented in Table 22. The dimension of the reduced system

Sampling	ROM dim	μ	4th EV(FEM)	4th EV(ROM)	Rel. Error(λ_4)
25	39	(0.5,0.6)	235.80616993	235.80620424	1.4×10^{-7}
		(0.5,0.8)	173.56836538	173.56838242	9.8×10^{-8}
		(0.8,0.6)	125.56104288	125.56109105	3.8×10^{-7}
		(0.8,0.8)	94.35030619	94.35032541	2.0×10^{-7}
49	40	(0.5,0.6)	235.80616993	235.80619246	9.5×10^{-8}
		(0.5,0.8)	173.56836538	173.56837272	4.2×10^{-8}
		(0.8,0.6)	125.56104288	125.56107025	2.1×10^{-7}
		(0.8,0.8)	94.35030619	94.35032558	2.0×10^{-7}

Table 21: Approximation of λ_4 with snapshot based on u_1, u_2, u_3, u_4 : comparison of FEM and ROM.

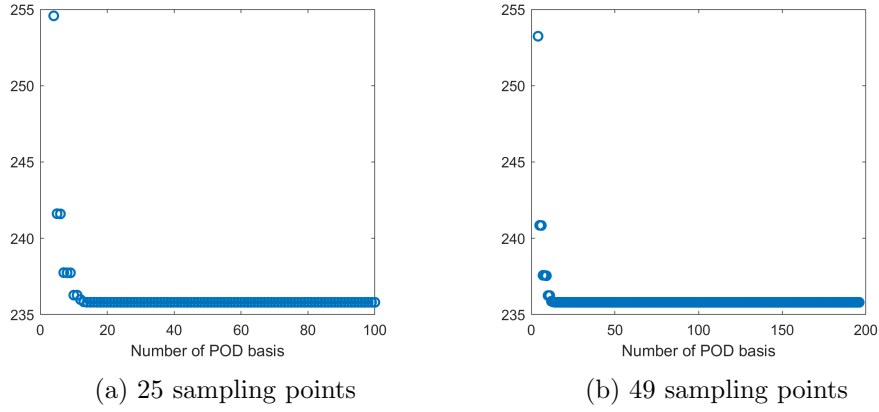


Figure 48: Approximation of λ_4 at $\mu = (0.5, 0.6)$ with snapshot based on u_1, u_2, u_3, u_4 : varying the number of POD basis.

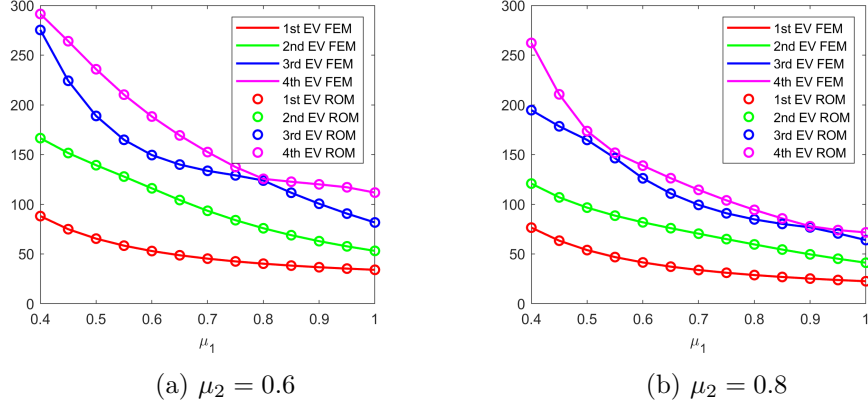


Figure 49: Approximation of $\lambda_1, \lambda_2, \lambda_3, \lambda_4$ with snapshot based on $u_1 + u_2 + u_3 + u_4$: comparison of FEM and ROM eigenvalues with varying μ_1 and fixed μ_2 , and 49 sample points.

Sampling	ROM dim	μ	4th EV(FEM)	4th EV(ROM)	Rel. Error(λ_4)
25	24	(0.5,0.6)	235.80616993	235.80707671	3.8×10^{-6}
		(0.5,0.8)	173.56836538	173.57125574	1.6×10^{-5}
		(0.8,0.6)	125.56104288	125.56717711	4.8×10^{-5}
		(0.8,0.8)	94.35030619	94.35107680	8.1×10^{-6}
49	40	(0.5,0.6)	235.80616993	235.80631238	6.0×10^{-7}
		(0.5,0.8)	173.56836538	173.56860618	1.3×10^{-6}
		(0.8,0.6)	125.56104288	125.56118125	1.1×10^{-6}
		(0.8,0.8)	94.35030619	94.35036064	5.7×10^{-7}

Table 22: Approximation of λ_4 with snapshot based on $u_1 + u_2 + u_3 + u_4$: comparison of FEM and ROM.

obtained using the criterion (3.10) is also mentioned in the same table. The maximum relative error among the four test points is 10^{-5} . We have shown the plot for the fourth eigenvalue of ROM at the point (0.5,0.6) with the different ROM dimensions in Figure 48 and one can see that the ROM eigenvalue is converging to the exact eigenvalue when the ROM dimension is more than 10. We use the sum of four eigenvectors we preserve the order of the eigenvalues of ROM and FOM at a price of getting a relative error which is higher than in the case where we use all the eigenvectors.

References

- [1] M. M. Alghamdi, F. Bertrand, D. Boffi, F. Bonizzoni, A. Halim, and G. Priyadarshi. On the matching of eigensolutions to parametric partial differential equations. In *eccomas2022*. 2022. URL: https://www.scipedia.com/public/Alghamdi_et_al.2022a.
- [2] M. M. Alghamdi, D. Boffi, and F. Bonizzoni. A greedy MOR method for the tracking of eigensolutions to parametric elliptic pdes. arXiv:2208.14054 [math.NA], 2022.
- [3] Fleurianne Bertrand, Daniele Boffi, and Abdul Halim. A reduced order model for the finite element approximation of eigenvalue problems. *Comput. Methods Appl. Mech. Engrg.*, 404:Paper No. 115696, 2023.

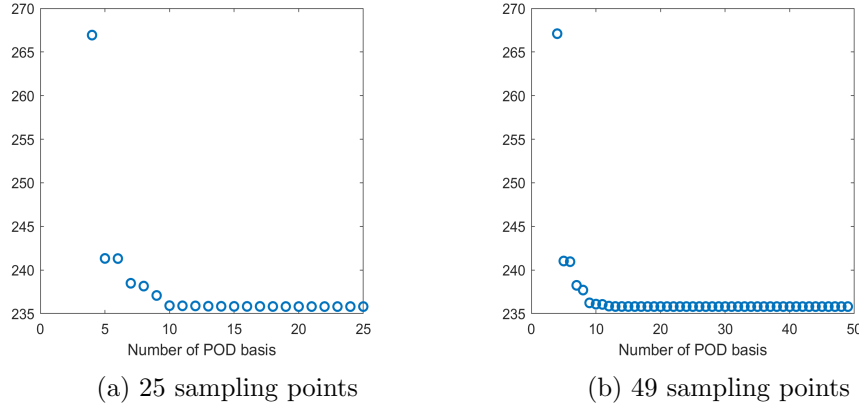


Figure 50: Approximation of λ_4 at $\mu = (0.5, 0.6)$ with snapshot based on $u_1 + u_2 + u_3 + u_4$: varying the number of POD basis.

- [4] A.G. Buchan, Christopher Pain, and Ionel Navon. A POD reduced order model for eigenvalue problems with application to reactor physics. *International Journal for Numerical Methods in Engineering*, 95(12):1011–1032, 2013.
- [5] I. Fumagalli, A. Manzoni, N. Parolini, and M. Verani. Reduced basis approximation and a posteriori error estimates for parametrized elliptic eigenvalue problems. *ESAIM: Mathematical Modelling and Numerical Analysis*, 50(6):1857 – 1885, 2016.
- [6] Niklas Georg, Wolfgang Ackermann, Jacopo Corno, and Sebastian Schöps. Uncertainty quantification for Maxwell’s eigenproblem based on isogeometric analysis and mode tracking. *Comput. Methods Appl. Mech. Engrg.*, 350:228–244, 2019.
- [7] P. German and J. C. Ragusa. Reduced-order modeling of parameterized multi-group diffusion k-eigenvalue problems. *Annals of Nuclear Energy*, 134:144–157, 2019.
- [8] J. Hesthaven, G. Rozza, and B. Stamm. *Certified Reduced Basis Methods for Parametrized Partial Differential Equations*. Springer International Publishing, Bilbao, 2016.
- [9] T. Horger, B. Wohlmuth, and T. Dickopf. Simultaneous reduced basis approximation of parameterized elliptic eigenvalue problems. *ESAIM: M2AN*, 51(2):443–465, 2017.
- [10] L. Machiels, Y. Maday, I. B. Oliveira, A. T. Patera, and D. V. Rovas. Output bounds for reduced-basis approximations of symmetric positive definite eigenvalue problems. *Comptes Rendus de l’Académie des Sciences - Series I - Mathematics*, 331(2):153–158, 2000.
- [11] Y. Maday, A. T. Patera, and J. Peraire. A general formulation for a posteriori bounds for output functionals of partial differential equations; application to the eigenvalue problem. *Comptes Rendus de l’Académie des Sciences - Series I - Mathematics*, 328(9):823–828, 1999.
- [12] G.S.H. Pau. Reduced-basis method for band structure calculations. *Phys. Rev. E*, 76:046704, 2007.
- [13] G.S.H. Pau. *Reduced basis method for quantum models of crystalline solids*. Ph.D. thesis, Massachusetts Institute of Technology, 2008.

- [14] G.S.H. Pau. Reduced basis method for simulation of nanodevices. *Physical Review B*, 78:155425, 2008.
- [15] C. Prud'homme, Rovas D.V., Veroy K., and Patera A.T. A mathematical and computational framework for reliable real-time solution of parametrized partial differential equations. *ESAIM: Mathematical Modelling and Numerical Analysis - Modélisation Mathématique et Analyse Numérique*, 36(5):747–771, 2002.
- [16] C. Prud'homme, D. V. Rovas, K. Veroy, L. Machiels, Y. Maday, A.T. Patera, and G. Turinici. Reliable Real-Time Solution of Parametrized Partial Differential Equations: Reduced-Basis Output Bound Methods . *Journal of Fluids Engineering*, 124(1):70–80, 2002.
- [17] A. Quarteroni, A. Manzoni, and F. Negri. *Reduced basis methods for partial differential equations: An introduction*. Springer, 2016.